Geoscience Frontiers 15 (2024) 101865

Contents lists available at ScienceDirect

Geoscience Frontiers

journal homepage: www.elsevier.com/locate/gsf

Research Paper

Frontier of the Paleo-Tethys Ocean in the western Mediterranean: Isotopic (Sm-Nd) constraints on sources of Devonian units from Menorca Island

Ricardo Arenas [a,*], José M. Fuenlabrada [b], Cristian Timoner [c], Rubén Díez Fernández [d], Esther Rojo-Pérez [a]

[a] Departamento de Mineralogía y Petrología and Instituto de Geociencias (UCM, CSIC), Universidad Complutense, Madrid, Spain
[b] Unidad de Geocronología (CAI de Ciencias de la Tierra y Arqueometría), Universidad Complutense, Madrid, Spain
[c] Bayerisches Geoinstitut, University of Bayreuth, Bayreuth, Germany
[d] Instituto Geológico y Minero de España – CSIC, Salamanca, Spain

ARTICLE INFO

Article history:
Received 13 October 2023
Revised 8 April 2024
Accepted 9 May 2024
Available online 10 May 2024
Handling Editor: S. Glorie

Keywords:
Western Paleo-Tethys frontiers
Menorca Island
Sm-Nd isotopic constraints
Devonian sequence
provenance in Gondwana

ABSTRACT

The c. 1000-m-thick pre-orogenic Devonian mainly metapelitic sequence of North Menorca Island shows a fairly complete stratigraphic succession. The rocks of this sequence indicate gradually increasing deeper marine conditions of sedimentation towards its uppermost levels. Furthermore, the obtained sedimentary characteristics resemble those related to a deep and narrow basin-associated deposit. Thin sills of Ti-augite-bearing alkaline gabbros occur within the Devonian sequence. The intensity of Variscan deformation increases downwards through the structure. According to the characteristics of the Devonian sequence and its location within the Variscan Orogen, a correlation with similar units located in the southern sectors of the Central Iberian Zone (Iberian Massif) is suggested. The Devonian metapelitic rocks have geochemical characteristics suggesting that they represent moderately recycled mature siliciclastic sediments, generated from erosion of distant source areas belonging to an upper continental crust. The relatively narrow range of variation observed in initial $^{143}Nd/^{144}Nd$ ratios supports a similar source for the Menorcan slates (0.51165–0.51182). However, a marked trend is observed in these isotope ratios, from lower values at the base of the stratigraphic column (minimum value of 0.511941) to higher values at the top (maximum value of 0.512131). The $^{147}Sm/^{144}Nd$ ratios vary between 0.1074 and 0.1238, within the range defined for siliciclastic rocks with felsic crustal provenance. The Nd model ages define a narrow range between 1496 Ma and 1754 Ma (Late Paleoproterozoic–Early Mesoproterozoic), and they are consistently younger up-section. These data rule out a provenance from the erosion of the West Africa Craton, as they are more compatible with a provenance from regions located in the Trans-Saharan Belt or Sahara Metacraton. The characteristics of the Menorcan Devonian sequence are compatible with its deposition in a narrow and deep *peri*-Gondwanan transtensional basin, generated to the south of an advancing Variscan orogenic wedge. Systematic variations in the Nd isotopic composition indicate the progressive and continuous denudation of increasingly more easterly North African sectors in a collisional context between Laurussia and Gondwana with a marked dextral component. These data must be interpreted in the sense that there was not a large oceanic domain during Devonian times to the south of Iberia, able to block the arrival of detrital material from North Africa. A large tract of the Paleo-Tethys Ocean would therefore not have existed during the Devonian south of Iberia. This ocean must therefore have had limited extent in this period towards the westernmost sectors. The Devonian *peri*-Gondwanan shelf was apparently continuous around Iberia. This platform was progressively affected by Variscan deformation advancing from north to south and incorporated into the Variscan orogenic wedge with the same vergence.

1. Introduction

The existence of a large Paleo-Tethys Ocean during Late Paleozoic times has been proposed by Stampfli and Borel (2002) and

* Corresponding author.
E-mail address: rarenas@ucm.es (R. Arenas).

https://doi.org/10.1016/j.gsf.2024.101865

Stampfli et al. (2013). Its opening would have taken place during most of the Devonian and its extension would occupy the entire northern *peri*-Gondwanan domain (Criniti, 2023; Criniti et al., 2023). The closure of the Paleo-Tethys Ocean would have essentially taken place during the Triassic and Early Jurassic, favoring different collisional events related to the formation of Central Asia. In turn, a new ocean opened to the south, the Neotethys Ocean (Stampfli and Borel, 2002; Critelli, 2018; Critelli and Martín-Martín, 2022, 2024). The actual extension of the Paleo-Tethys Ocean in the western domains north of NW Africa is difficult to constrain, since this region was affected from the Lower Devonian onwards by the frontal collision between Gondwana and Laurussia that assembled Pangea and gave rise to the Variscan Orogen (Critelli and Reed, 1999; Criniti et al., 2023; Costamagna and Criniti, 2024). Determining the existence of the Paleo-Tethys Ocean in these regions is a key issue in understanding the dynamics of the lithospheric plates, the development of sedimentary sequences and even the possible existence of volcanic arcs capable of explaining the Variscan granitic magmatisms of Southern Europe (Pereira et al., 2015). However, to advance this issue, it is also critical to understand the characteristics of the Variscan Orogen in this region.

The Variscan Orogen extends through Europe and NE Africa and continues across the Atlantic Ocean in the Appalachian Orogen (Matte, 1991; Hatcher, 2010; Kroner and Romer, 2013; Franke et al., 2017; Martínez Catalán et al. al., 2009, 2020; Schulmann et al., 2022). The collision of Gondwana with Laurussia was complex and led to the closure of the Paleozoic Rheic Ocean (Nance et al., 2010) and the opening and closure of minor oceanic domains (Arenas et al., 2014, 2016; Díez Fernández et al., 2016; Criniti et al., 2023). Most of the continental crust involved in the Variscan Orogen was derived from the African margin of the Gondwana supercontinent. However, the development of the orogen and the intensity and complexity of the associated deformation greatly hinders the establishment of correlations throughout the orogen and with the different equivalent continental sections, which are currently distributed across North Africa. This difficulty is also increased by the opening of the Mediterranean Sea during the Mesozoic (Alpine-Tethys Ocean; Stampfli and Borel, 2002), which prevents the cartographic continuity of the terranes located on its European and African shores (Critelli et al., 2018; Kairouani et al., 2023).

The correlation of Variscan terranes with their possible African equivalents must therefore be approached using indirect methods. The U-Pb geochronology of detrital zircons and Sm-Nd systematics make it possible to establish some correlations. The U-Pb geochronology of detrital zircons makes it possible to recognize the provenance of siliciclastic sequences from the West African Craton (WAC) or the Sahara Meta-Craton (SMC) and Arabian-Nubian Shield (ANS). The increase in the abundance of Mesoproterozoic zircons is considered a criterion for more eastern provenances. These zircons are virtually absent in the Ediacaran and Cambrian sequences with source areas located in the northern regions of the WAC (Díez Fernández et al., 2010; Linnemann

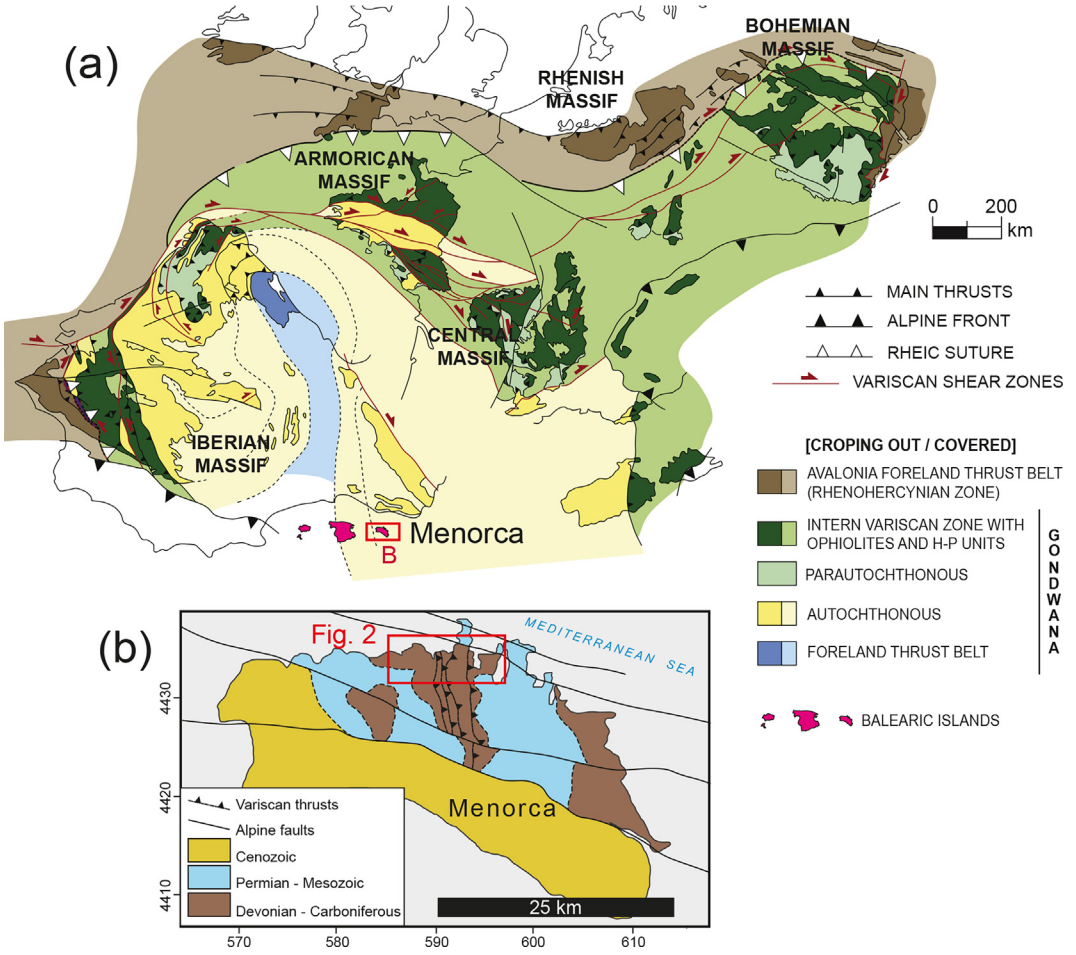

Fig. 1. (a) Terrane distribution in the Variscan Orogen. (b) Geology of Menorca Island.

et al., 2011, 2014; Avigad et al., 2012, 2022; Pereira et al., 2012, 2017; Fernández Suárez et al., 2014; Albert et al., 2015a, 2015b). The Nd model ages (T_{DM}) make it possible to obtain average whole rock values from the original isotopic signatures (Linnemann and Romer, 2002). Siliciclastic rocks derived from the erosion of the WAC record older T_{DM} values than those whose source areas are the SMC or the ANS (Fuenlabrada et al., 2020). Using the Sm-Nd methodology and an extensive database, it is possible, for example, to recognise and differentiate isotopic signatures during the Ediacaran and Early Cambrian periods from the *peri*-Gondwanan shelves located on both sides of the Trans-Saharan Belt (Fuenlabrada et al., 2023).

In the western sector of the Mediterranean Sea, Menorca Island (Balearic Islands, Fig. 1) contains a section of Paleozoic basement whose age ranges from the Silurian-Devonian boundary to the Permian (Bourrouilh, 1983; Rosell et al., 1987a, 1987b). The Devono–Carboniferous sequence of the central part of the island is pre-orogenic, has an uncertain correlation and is affected by Variscan deformation with poorly known tectonothermal evolution. The eastern part of the island contains a *syn*-orogenic Kulm Facies Carboniferous sequence. This Paleozoic basement represents one of the southernmost preserved sections of the Variscan orogen and its isolation makes it difficult to establish correlations with other terranes of the Iberian Massif or other *peri*-Mediterranean coeval sections (Sabat et al., 2018). However, the characteristics and meaning of the Menorcan basement are important for correlations in the Ibero-Armorican arc and for the development of the Variscan Orogen and the oceanic domains involved. On the other hand, the original location of the Menorcan basement at the Gondwanan margin has only recently been investigated based on the U-Pb geochronology of detrital zircons (Martinez et al., 2016; Cristóbal et al., 2023), although these U-Pb data were obtained only in the Carboniferous sequence and no other isotopic data have been published. Whole-rock geochemical data can advance the knowledge of the initial paleogeographic context. This work presents new whole-rock elemental and isotopic geochemical (Sr, Nd) data from the Devonian sequence of central Menorca. The information provided by these new geochemical data, together with other new data on the stratigraphy, structure, and tectonothermal evolution of the Paleozoic units, will be used to discuss the origin of this basement on the Gondwana margin, its correlation throughout the Ibero-Armorican arc, its orogenic evolution, and the characteristics of the Paleo-Tethys Ocean during the deposition of the Devonian sequence.

2. Geological setting

2.1. Structure and metamorphism

The investigated pre-orogenic basement crops out in the northern sector of Menorca Island (Fig. 1). It is made up of a c. 2500-m-thick Devonian and Carboniferous stratigraphic sequence (Fig. 2). This sequence presents low-grade metamorphic conditions that increases from east to west. The upper levels of the stratigraphic sequence contain shale layers that progressively change to slates that show a well-defined regional schistosity (S_1). The deeper structural levels contain phyllites, with S_1 developed by the orientation of white mica and chlorite lepidoblasts (chlorite zone; García et al., 1992). The structural evolution is characterised by the development of a sequence of W-directed thrust sheets, synchronous with the development of S_1 (Tramuntana thrust sheet). This structure is compatible with the position of Menorca Island on the eastern flank of the Ibero-Armorican arc (Fig. 1), which entails the rotation of the Variscan structures from an initial vergence towards the East. Ductile deformation associated with this stacking increases towards the base (Binimel-lá, Fig. 2). There is a hectometric basal shear zone characterised by overturned folds with sheared flanks. This imbricated sequence has previously been described as an olistostromal complex, devoid of ductile deforma-

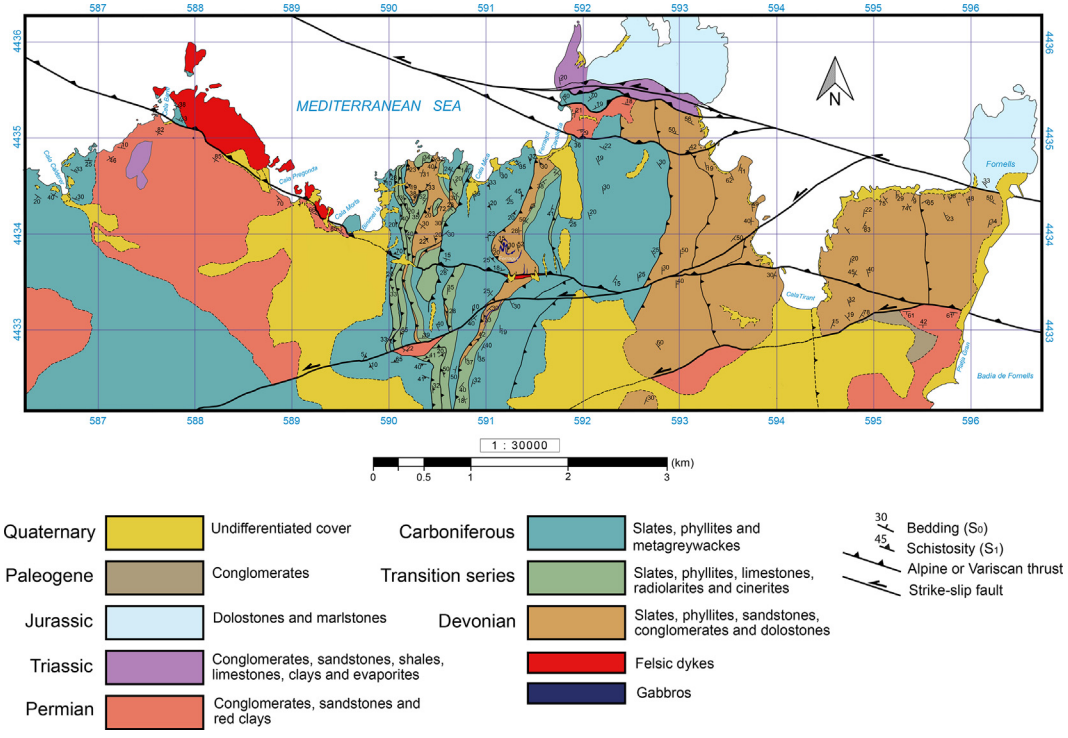

Fig. 2. Geological map of north central Menorca Island.

tion and metamorphism (Rosell et al., 1987a; Card and Mortenari, 2023). The S_1 regional schistosity is affected by upright folds. The metamorphic basement is covered by Mesozoic and Cenozoic strata (Fig. 2), which are affected by Alpine folds and NE–SW and NW–SE trending faults with dominant left-lateral movement (Timoner et al., 2021).

2.2. Devonian and Carboniferous stratigraphy

Fig. 3 shows the general stratigraphic column of central Menorca basement. This synthetic column has been compiled based on data provided by Bourrouilh (1983) and own stratigraphic and paleontological observations. The Devonian sequence is characterised by heterogeneous turbidites ranging from quartzites to calcarenite sandstones, gradually transitioning to deeper marine environments towards the uppermost Devonian. The Early to Middle Devonian sequence consists of alternations of shales, slates and quartz arenites, hybrid sandstones and calcarenites with local slumps and turbiditic channels (Fig. 4). These display up to four cyclic sequences of enrichment in carbonate of 125 m from the Pragian to the Givetian. The lowest levels of the Devonian sequence are represented by an alternation of thin-bedded sand-

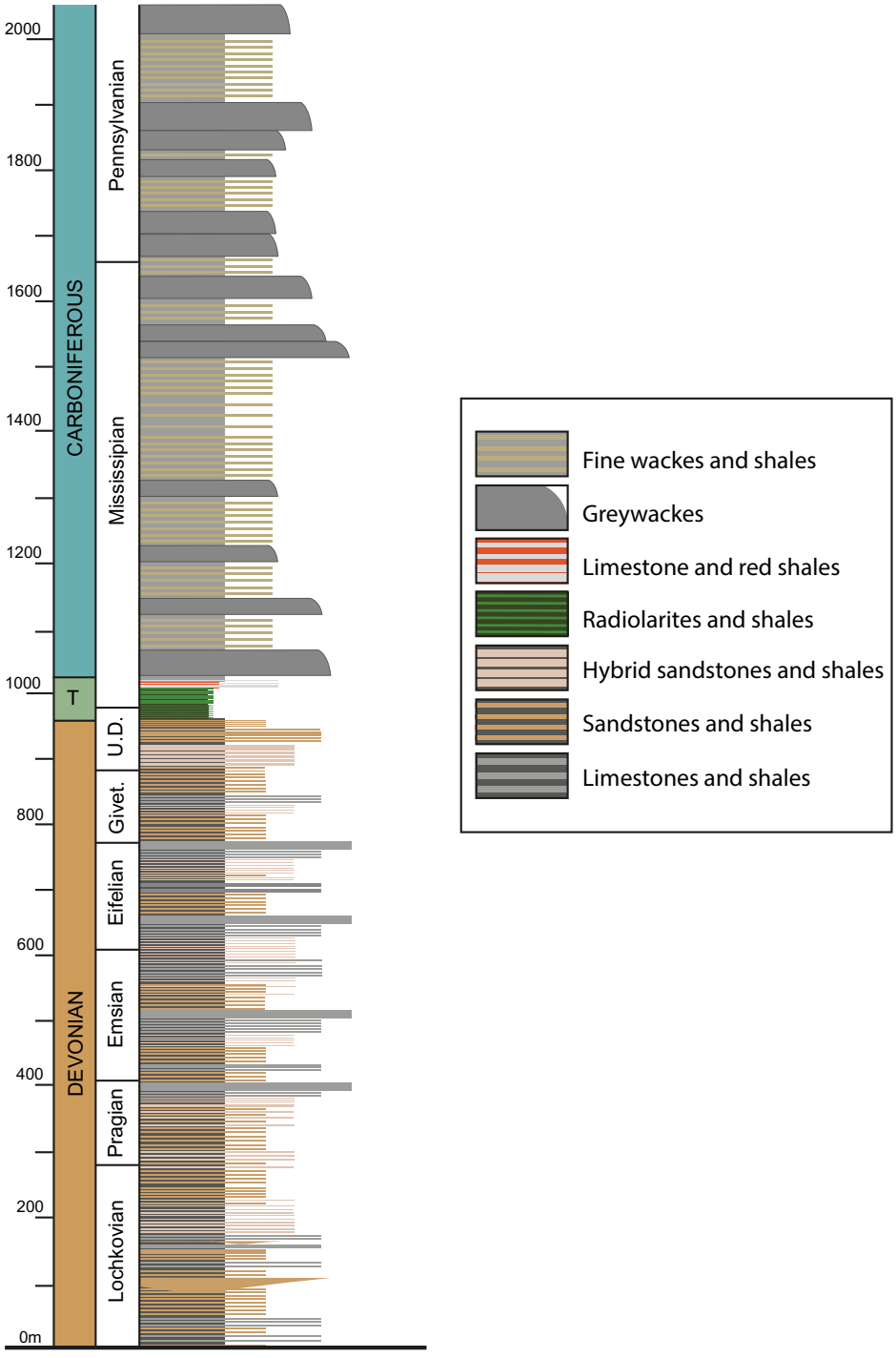

Fig. 3. Synthetic stratigraphic column of Devonian and Carboniferous sequences of north central Menorca. U.D., Upper Devonian; T, transition sequences. Based on Bourrouhil (1983) and own data.

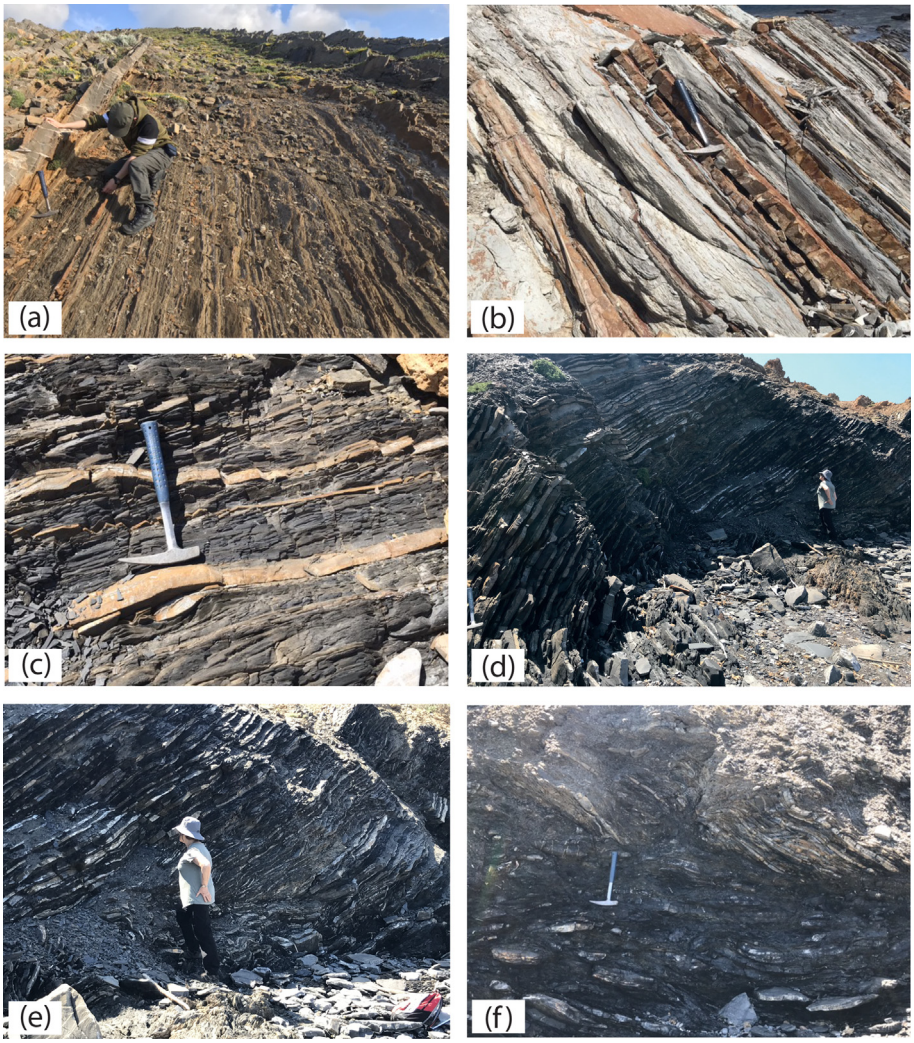

Fig. 4. (a) Devonian sequence in the coastal section west of Fornells. (b) Alternation of slates and sandstones in Lochkovian sequence near Cala Tirant. (c–f) Outcrops of lowest Devonian sequence, transitioning to Silurian, in Cala Tirant. It is made up of rhythmic alternations of thin levels of sandstone and black slate. It is affected by metre-thick ductile shear zones suggesting that this sequence is detached on its substrate and not observable on Menorca Island.

stones and black slates with graptolites only appearing in Cala Tirant. This sedimentary sequence is highly deformed and affected by intense local shearing (Fig. 4), and it was considered by Bourrouilh (1983) to be of Upper Silurian age. The age of this lowest Devonian sequence was established using graptolites and conodonts (Bourrouilh, 1983). The upper section of the Givetian shows a clear enrichment in shales as well as a drastic decrease in the sedimentation rate. The Upper Devonian consists of a total of 40 m alternating black shales and fine-grained sandstones with episodic turbidites composed of dolomitic sandstone with pyrite, and nodules of iron and manganese oxide. The Devonian sequence culminates with three coarse-grained terrigenous layers. The age of the Upper Devonian sequence has been obtained using conodonts by Tiedt (1994) and Bourrouilh (1983). The Uppermost Devonian, Tournaisian and Visean correspond to 40 m of radiolarites, followed by 10 m of alternating red clays and mudstone representing a pelagic environment (Card and Montenary, 2023; Fig. 3). On top of the red clays, the Carboniferous sequence is composed of a thick alternation of grey shales, greywackes and conglomerates deposited in a foredeep basin (Rosell and Arribas, 1989). The Devonian sedimentary sequence therefore contains a fairly complete stratigraphic record with a thickness of c. 1000 m (Fig. 3). This sequence would have been deposited in a strait-like narrow basin (Card and Montenary, 2023). The c. 3000-m-thick eastern Menorcan Carboniferous sequence contains a *syn*-orogenic greywackic flysch equivalent to the Kulm-type Carboniferous sequence of other regions of the Variscan orogen (Rosell et al., 1987a, 1987b).

2.3. Igneous rocks

The Upper Devonian sequence is intruded by at least four thin mafic dykes (a few metres thick), the Tramuntana Gabbros (TG). They are deformed sills cropping out between Variscan thrusts in the area of Binimel-là, near Ferragut Vell and Ferragut Nou. The TG are composed of isotropic gabbros, and they show evidence of being emplaced at the base of the radiolarites. They are alkaline types containing Ti-rich augitic clinopyroxene. These mafic dykes were mapped by Bourrouhil (1983), who described the rocks as alkaline spilites consisting of submarine lavas and dykes. Other igneous rocks cropping out in this region include thick felsic dykes of Carboniferous–Permian age (Fig. 2).

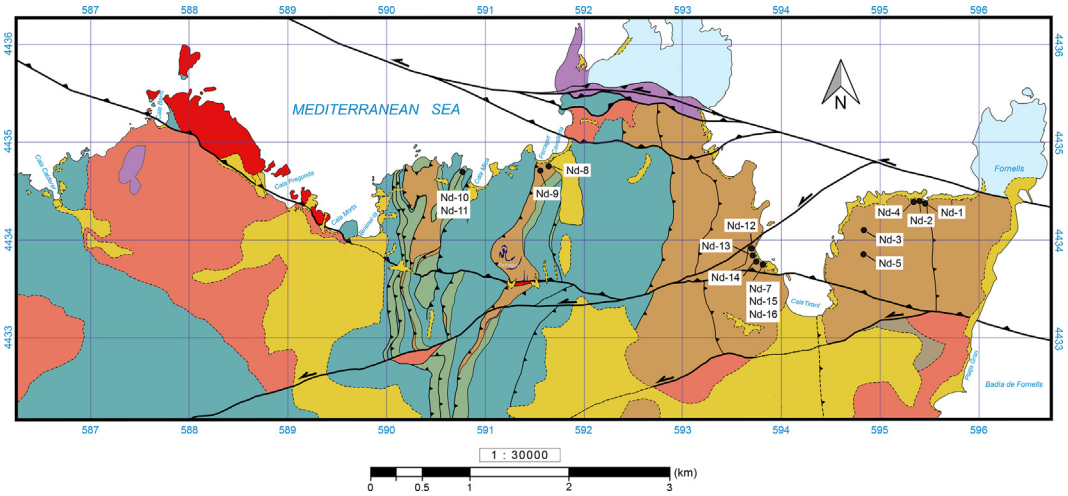

Fig. 5. Location of samples used for elemental and isotope geochemistry.

3. Whole-rock geochemistry

3.1. Methodology

Fifteen representative samples of Devonian and Early Carboniferous slates were selected for both elemental and isotopic (Sr-Nd) whole-rock geochemistry. They were all collected near a coastal section, between the western part of Fornells and Cala Mica (Fig. 5). Samples Nd-13 to Nd-16 correspond to the lowest levels of the Devonian sequence, in the transition to the Silurian described by Bourrouhil (1983) (Fig. 4). Collectively, the sampled metapelites span the entire Devonian sequence, including the red transitional Viseean layers analysed by Card and Montenary (2023) (Fig. 6).

3.1.1. Elemental geochemistry

Crushed and powdered rock samples at Universidad Complutense de Madrid (Spain) were used for geochemical and isotopic analysis. The major and trace elements were analysed at Activation Laboratories Ltd (Actlabs, Ontario, Canada) using a sample dissolution process that consisted of alkaline fusion with lithium metaborate/tetraborate. The analytical method used for the major elements and Sc, Be, V, Zr, Ba, and Sr was ICP-OES, while ICP-MS was used for the rest of the trace elements. The quality of the performed analyses is high, with a detection limit of $\sim$ 0.01% for most of the major elements and a detection limit of $\sim$ 0.001% for MnO and TiO_2; for trace elements, the detection limit varied from 0.002 ppm for Lu to 30 ppm for Zn. The detection limits for each element, the composition of the standards used for the analyses, and the analytical details of each element can be found in Arenas et al. (2021). The major and trace element contents are shown in Table 1.

3.1.2. Sr-Nd isotopic geochemistry

Nd-Sr isotope determinations were performed at the Geochronology Facility of Universidad Complutense de Madrid (https://cai.ucm.es/en/earth-sciences-archeometry/geochronology/), using a thermal ionization mass spectrometer (TIMS). Previously weighed samples were dissolved in a pressure environment with HF-HNO_3-HCl (Merck-Suprapur® ultraclean reagents). The resulting solutions were passed through a double-step chromatographic separation: (i) DOWEX AG®50x8 200–400 mesh resin (Bio-Rad Laboratories, Inc, USA) was used in order to separate the Sr (Rb-free) fraction and the complete rare earth element (REE) group from the bulk matrix of the sample; and (ii) LnResin®

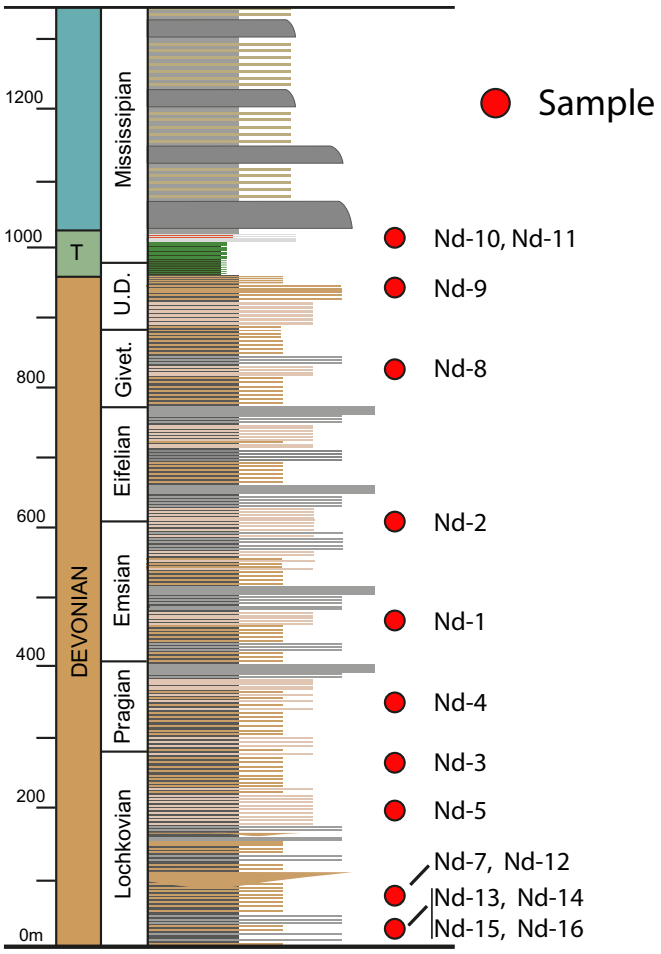

Fig. 6. Stratigraphic location of samples used for elemental and isotope geochemistry. The chronostratigraphy of the Devonian sequence is based on the work of Bourrouhil (1983) and our own data.

Table 1
Whole rock major and trace element data of Devonian metasedimentary slates from Menorca Island.

	Nd-1	Nd-2	Nd-3	Nd-4	Nd-5	Nd-7	Nd-8	Nd-9	Nd-10	Nd-11	Nd-12	Nd-13	Nd-14	Nd-15	Nd-16
SiO_2	60.45	62.62	46.85	62.93	59.01	50.72	46.01	54.52	52.25	51.22	58.68	45.95	49.7	53.44	52.91
Al_2O_3	18.87	16.25	18.06	16.4	13.62	22.93	17.2	18.89	18.65	20.8	15.42	25.67	20.69	13.61	19.95
Fe_2O_3	2.61	4.84	8.87	4.62	4.88	6.34	6.94	7.39	7.59	10.25	4.26	7.03	6.91	7.59	6.06
MnO	0.028	0.071	0.077	0.131	0.105	0.035	0.083	0.059	0.123	0.341	0.051	0.026	0.065	0.059	0.046
MgO	1.65	1.6	2.08	1.38	2.65	1.53	2.83	1.1	1.23	1.68	3.64	1.86	2.69	2.55	3.01
CaO	1.06	0.32	5.07	0.16	3.45	0.62	6.25	2.01	4.23	0.83	2.5	0.65	2.49	7.86	2.82
Na_2O	1.75	0.74	0.47	1.86	0.19	1.23	0.76	0.62	0.9	0.58	1.43	0.85	0.85	0.75	0.78
K_2O	5.05	4.81	5.36	4.5	3.33	3.66	2.95	3.8	4.61	5.18	3.39	4.02	3.76	2	4.09
TiO_2	1.64	0.787	0.809	0.94	0.727	0.921	0.84	1.022	0.658	0.795	0.798	1.084	0.932	0.694	0.977
P_2O_5	0.2	0.13	0.15	0.11	0.23	0.14	0.14	0.13	0.11	0.16	0.13	0.12	0.13	0.66	0.13
LOI[1]	5.61	6.18	11.45	5.51	10.11	11.99	14.58	8.65	8.71	7.2	10.31	11.58	10.36	11.13	9.7
Total	98.91	98.34	99.26	98.55	98.31	100.1	98.56	98.17	99.06	99.03	100.6	98.85	98.59	100.3	100.5
Sc	20	17	22	15	14	20	16	17	19	22	13	26	21	13	19
Be	4	4	5	4	3	4	3	4	3	4	3	5	5	2	5
V	182	130	137	131	132	189	114	136	125	170	100	189	347	131	182
Cr	130	100	110	90	90	130	90	100	90	120	80	160	140	80	120
Co	15	18	39	22	24	30	22	22	45	50	20	27	20	19	23
Ni	20	70	70	70	70	100	40	40	140	130	50	60	80	60	60
Cu	70	60	100	60	60	60	50	40	30	20	60	40	70	40	60
Zn	80	140	260	160	190	160	110	120	80	100	90	130	220	160	110
Ga	25	24	27	22	19	30	26	26	24	28	25	44	33	20	34
Ge	1.5	1.4	1.7	1.6	1.7	0.9	1.7	1.8	2.1	2.3	1.7	1.5	0.9	0.9	1
As	< 5	< 5	6	18	12	< 5	5	6	16	< 5	< 5	< 5	5	9	< 5
Rb	171	180	214	161	128	193	133	162	193	224	154	223	209	108	220
Sr	90	75	194	126	385	315	357	325	186	267	464	352	130	248	143
Y	29	23.2	31.4	31.1	30.9	25.8	30.2	30.7	24.6	34	28.6	29	18.2	33.9	27
Zr	348	121	208	284	199	106	150	333	126	133	235	88	123	230	192
Nb	32.4	16.1	24.2	19	13.8	17.1	21.7	23.4	12.6	12.6	19.3	22.3	18.4	14.1	21.3
Mo	< 2	< 2	< 2	2	< 2	2	< 2	< 2	< 2	< 2	< 2	< 2	3	5	3
Ag	< 0.5	< 0.5	< 0.5	< 0.5	< 0.5	< 0.5	< 0.5	< 0.5	< 0.5	< 0.5	< 0.5	< 0.5	< 0.5	< 0.5	< 0.5
In	0.1	0.1	0.1	0.1	0.1	0.1	0.1	0.1	0.1	0.1	0.1	0.1	0.1	< 0.1	0.1
Sn	3	3	4	3	2	2	3	3	3	4	3	4	3	2	3
Sb	< 0.2	0.2	0.5	1.4	0.4	0.6	< 0.2	< 0.2	1.4	0.7	0.2	0.2	1.5	1.8	0.4
Cs	4.2	9.3	16.8	5.4	9.3	8.8	9.4	9.3	12.7	12.4	7.8	10.5	8.4	4.2	9.3
Ba	579	567	450	564	427	604	233	1387	569	712	793	691	595	397	748
La	55.4	47.2	58.8	52.8	48.9	50.9	52.9	59.5	42.9	48.1	45.3	71.9	45.2	39.7	52
Ce	108	87.4	105	107	96.6	89.9	98	113	119	113	85.3	130	74.7	72.1	94.5
Pr	12.1	10.1	11.8	11.4	12.3	10.3	11.4	12.8	9.77	11.2	9.57	15	8.71	8.54	11.1
Nd	44.9	37.2	43.2	43.9	47	37.9	42.9	47.5	36.3	42.8	36	54	33.2	33.4	41.4
Sm	8.33	6.61	7.88	8.3	9.22	7.21	8.49	8.94	7.28	8.62	6.81	10.2	5.92	6.84	7.7
Eu	1.58	1.23	1.52	1.52	1.8	1.52	1.68	1.74	1.41	1.84	1.26	1.84	1.05	1.57	1.39
Gd	6.44	5.3	6.5	6.99	7.58	5.81	7.08	7.12	5.69	7.47	5.51	6.6	3.61	6.17	5.52
Tb	0.96	0.78	1.01	1.05	1.09	0.84	1.07	1.04	0.9	1.17	0.85	0.98	0.55	0.99	0.88
Dy	5.61	4.48	6.11	6.07	5.94	4.93	5.96	6.22	5.1	6.82	5.08	5.53	3.23	5.84	5.07
Ho	1.13	0.84	1.22	1.19	1.09	0.99	1.14	1.17	0.98	1.29	0.97	1.07	0.66	1.1	1
Er	3.19	2.35	3.61	3.29	3.05	2.81	3.12	3.49	2.83	3.71	2.83	3.07	2.05	3.15	2.95
Tm	0.463	0.337	0.531	0.485	0.425	0.408	0.438	0.498	0.417	0.524	0.439	0.475	0.307	0.446	0.454
Yb	3.19	2.13	3.37	3.16	2.59	2.57	2.92	3.28	2.75	3.46	2.91	3.22	1.96	2.95	2.97
Lu	0.508	0.323	0.536	0.492	0.407	0.395	0.46	0.497	0.432	0.538	0.48	0.521	0.319	0.427	0.438
Hf	8.1	2.9	5	6.3	4.8	2.6	3.8	8.1	3.3	6.5	6.7	2.7	3.4	6.1	5.6
Ta	2.38	1.39	1.78	1.54	1.13	1.2	1.58	1.72	0.95	1	1.38	1.49	1.29	0.97	1.44
W	5.7	4.3	6.6	14.4	9.2	7.9	12.9	5.1	4.9	3.4	43	7.4	10.6	35.4	32.8
Tl	0.73	0.69	0.96	0.62	0.77	0.75	0.69	0.78	0.94	1.27	0.47	0.9	1.05	0.71	0.96
Pb	23	37	104	87	317	14	17	25	27	21	22	10	10	12	10
Bi	0.2	< 0.1	0.4	0.3	< 0.1	< 0.1	< 0.1	0.2	1.1	0.8	0.1	< 0.1	< 0.1	< 0.1	< 0.1
Th	18.2	18	21	18.9	15.5	14.8	15.1	21.3	14.7	15.5	17.2	22.2	15.4	10.6	15.9
U	3.58	3.66	3.26	4.2	4.26	4.4	2.97	3.62	1.76	2.39	3.31	3.96	5.72	5.74	4.95
SiO_2/Al_2O_3	3.20	3.85	2.59	3.84	4.33	2.21	2.68	2.89	2.80	2.46	3.81	1.79	2.40	3.93	2.65
K_2O/Na_2O	2.89	6.50	11.40	2.42	17.53	2.98	3.88	6.13	5.12	8.93	2.37	4.73	4.42	2.67	5.24
Al_2O_3/TiO_2	11.51	20.65	22.32	17.45	18.73	24.90	20.48	18.48	28.34	26.16	19.32	23.68	22.20	19.61	20.42
Rb/Sr	1.90	2.40	1.10	1.28	0.33	0.61	0.37	0.50	1.04	0.84	0.33	0.63	1.61	0.44	1.54
Cr/Th	7.14	5.56	5.24	4.76	5.81	8.78	5.96	4.69	6.12	7.74	4.65	7.21	9.09	7.55	7.55
Cr/V	0.71	0.77	0.80	0.69	0.68	0.69	0.79	0.74	0.72	0.71	0.80	0.85	0.40	0.61	0.66
Sc/Th	1.10	0.94	1.05	0.79	0.90	1.35	1.06	0.80	1.29	1.42	0.76	1.17	1.36	1.23	1.19
Th/Sc	0.91	1.06	0.95	1.26	1.11	0.74	0.94	1.25	0.77	0.70	1.32	0.85	0.73	0.82	0.84
La/Sc	2.77	2.78	2.67	3.52	3.49	2.55	3.31	3.50	2.26	2.19	3.48	2.77	2.15	3.05	2.74
Co/Th	0.82	1.00	1.86	1.16	1.55	2.03	1.46	1.03	3.06	3.23	1.16	1.22	1.30	1.79	1.45
Zr/Sc	17.40	7.12	9.45	18.93	14.21	5.30	9.38	19.59	6.63	6.05	18.08	3.38	5.86	17.69	10.11
PIA[2]	75.59	88.13	56.00	78.88	62.40	87.08	53.29	77.20	60.53	87.96	64.08	90.29	74.75	45.08	71.79
ICV[3]	0.73	0.81	1.26	0.83	1.13	0.63	1.20	0.85	1.04	0.95	1.04	0.60	0.86	1.58	0.89
ΣREE	251.80	206.28	251.09	247.65	237.99	216.48	237.56	266.80	235.76	250.54	203.31	304.41	181.47	183.22	227.37
La_N/Yb_N	11.61	14.82	11.67	11.17	12.63	13.24	12.11	12.13	10.43	9.30	10.41	14.93	15.42	9.00	11.71

(*continued on next page*)

Table 1 (*continued*)

	Nd-1	Nd-2	Nd-3	Nd-4	Nd-5	Nd-7	Nd-8	Nd-9	Nd-10	Nd-11	Nd-12	Nd-13	Nd-14	Nd-15	Nd-16
Gd_N/Yb_N	1.61	1.98	1.54	1.76	2.33	1.80	1.93	1.73	1.65	1.72	1.51	1.63	1.47	1.67	1.48
Eu/Eu*	0.66	0.64	0.65	0.61	0.66	0.72	0.67	0.67	0.67	0.70	0.63	0.69	0.70	0.74	0.66

Oxides are in weight percent (wt.%).
Trace elements are in parts per million (ppm).
[1] Loss on ignition
[2] PIA (Plagioclase Index of Alteration; Fedo et al., 1995).
[3]ICV (Index of Compositional Variability; Cox et al., 1995).

Table 2
Whole rock Nd isotope data of metasedimentary rocks from Menorca Island.

Sample	Sm	Nd	$^{147}Sm/^{144}Nd$	$^{143}Nd/^{144}Nd$	±StErr*10^{-6}	$\varepsilon_{Nd(0)}$	$\varepsilon_{Nd(390\ Ma)}$	T_{DM} (Ma)[a]	$^{143}Nd/^{144}Nd$ initial
Nd-1	8.33	44.90	0.1121	0.512033	1	−11.8	−7.6	1513	0.511747
Nd-2	6.61	37.20	0.1074	0.511972	1	−13.0	−8.5	1533	0.511698
Nd-3	7.88	43.20	0.1103	0.511983	1	−12.8	−8.5	1560	0.511701
Nd-4	8.30	43.90	0.1143	0.511957	1	−13.3	−9.2	1662	0.511665
Nd-5	9.22	47.00	0.1186	0.512001	1	−12.4	−8.5	1667	0.511698
Nd-7	7.21	37.90	0.1150	0.512006	1	−12.3	−8.3	1599	0.511712
Nd-8	8.49	42.90	0.1196	0.512118	1	−10.1	−6.3	1496	0.511813
Nd-9	8.94	47.50	0.1138	0.512047	1	−11.5	−7.4	1517	0.511756
Nd-10	7.28	36.30	0.1212	0.512129	1	−9.9	−6.2	1505	0.511819
Nd-11	8.62	42.80	0.1217	0.512131	1	−9.9	−6.2	1509	0.511820
Nd-12	6.81	36.00	0.1143	0.511941	2	−13.6	−9.5	1688	0.511649
Nd-13	10.20	54.00	0.1142	0.512010	1	−12.3	−8.1	1580	0.511718
Nd-14	5.92	33.20	0.1078	0.511946	1	−13.5	−9.1	1577	0.511670
Nd-15	6.84	33.40	0.1238	0.512007	1	−12.3	−8.7	1754	0.511691
Nd-16	7.70	41.40	0.1124	0.511973	1	−13.0	−8.8	1607	0.511686

[a]Nd model ages (T_{DM}) calculated according to DePaolo (1981).
Decay constant for ^{147}Sm: 6.54×10^{-12} y^{-1} (Lugmair and Marti, 1978).
Present-day CHUR parameters: $^{147}Sm/^{144}Nd$ = 0.1967; $^{143}Nd/^{144}Nd$ = 0.512638 (Jacobsen and Wasserburg, 1980).
Sm and Nd contents from Table 1.

Table 3
Whole rock Sr isotope data of metasedimentary rocks from Menorca Island.

Sample	Rb	Sr	$^{87}Rb/^{86}Sr$	$^{87}Sr/^{86}Sr$	±StErr*10^{-6}	$\varepsilon_{Sr(390\ Ma)}$	$^{87}Sr/^{86}Sr$ inital
Nd-1	171	90	5.5134	0.737912	2	46.3	0.707294
Nd-2	180	75	6.9695	0.745513	3	39.4	0.706809
Nd-3	214	194	3.1972	0.725986	2	59.6	0.708231
Nd-4	161	126	3.7055	0.731330	3	95.4	0.710753
Nd-5	128	385	0.9627	0.715891	2	92.5	0.710544
Nd-7	193	315	1.7748	0.720088	2	88.0	0.710232
Nd-8	133	357	1.0792	0.715087	2	71.9	0.709094
Nd-9	162	325	1.4432	0.716184	2	58.7	0.708169
Nd-10	193	186	3.0046	0.723595	2	40.8	0.706909
Nd-11	224	267	2.4311	0.722680	1	73.1	0.709179
Nd-12	154	464	0.9617	0.715840	2	91.8	0.710499
Nd-13	223	352	1.8351	0.719903	2	80.6	0.709712
Nd-14	209	130	4.6633	0.733792	2	54.8	0.707895
Nd-15	108	248	1.2611	0.716586	2	78.8	0.709583
Nd-16	220	143	4.4618	0.732106	2	46.8	0.707328

Decay constant for ^{87}Rb: 1.42×10^{-11} y^{-1} (Steiger and Jäger, 1977).
Present-day CHUR parameters: $^{87}Rb/^{86}Sr$ = 0.085; $^{87}Sr/^{86}Sr$ = 0.7047 (after Caro and Bourdon, 2010).
Rb and Sr contents from Table 1.

(50–100 μm) resin (Eichrom Technologies, Lisle, IL, USA) was used for a complete separation of the Nd fraction from the Sm isotopes, following the methods described in Fuenlabrada (2023). Sr fractions were loaded along with 2 μL of ultrapure 1 M H_3PO_4 and 2 μL of Ta_2O_5, onto a pre-cleaned central Re ribbon. The analysis was performed in a Phoenix-TIMS (IsotopX) following a multi-dynamic collection method by keeping a stable 3 V ion beam intensity on the ^{88}Sr mass during a maximum of 160 replicas. $^{87}Sr/^{86}Sr$ ratios were corrected for possible ^{87}Rb interferences and normalised to the average $^{86}Sr/^{88}Sr$ value of 0.1194 (Nier, 1938). The final Sr isotope ratios were also corrected based on the isotopic Sr standard ratios (NBS 987 – Standard Reference Material 987) and analysed along with the samples; they yielded an average value of $^{87}Sr/^{86}Sr$ = 0.710248 (±0.000012; 2SD) for seven replicate analyses. In turn, the Nd (Sm-free) fractions were loaded, together with 2 μL ultrapure 0.05 M H_3PO_4, onto a lateral pre-cleaned Re

ribbon in a triple Re-ribbon arrangement. The analysis, performed in a Phoenix-TIMS (IsotopX), was followed by a multi-dynamic collection method. A stable intensity of 1 V in the ion beam of the ^{144}Nd mass was maintained during a maximum of 160 replicas. A regular correction of Nd isotope ratios for mass fractionation was carried out considering a normalised value of 0.7219 for the ^{146}Nd/^{144}Nd ratio (O'Nions et al., 1979). The potential presence of ^{142}Ce and ^{144}Sm isobaric interferences was continuously checked and corrected during the Nd isotope analysis. The Nd-isotope standard JNdi-1 (Tanaka et al., 2000) was run along with the Menorca slate samples for a final correction of the resulting ^{143}Nd/^{144}Nd ratios, yielding an average value for the ^{143}Nd/^{144}Nd ratio of 0.512105 (±0.000006; 2σ) for eight replicas. The analytical errors on the ^{87}Sr/^{86}Sr and ^{143}Nd/^{144}Nd ratios were estimated to be lower than 0.01% and 0.006%, respectively. The Sr and Nd procedural blanks were always < 0.5 ng and 0.1 ng, respectively. The results of the Nd and Sr isotopic analyses are given in Tables 2 and 3, respectively.

3.2. Results

3.2.1. Elemental geochemistry

No large variations among the samples are observed in the major elements. They present a relatively low SiO_2 abundance (avg. 53.82 wt.%) compared to those of the Post Archean Australian Shale (PAAS; Taylor and MacLennan, 1985) (62.80 wt.%). With the exception of CaO, the average values of the rest of major elements fit those of the average shale, which is compatible with a pelitic character of the Menorcan Devonian slates. The latter is confirmed by the SiO_2/Al_2O_3 and Al_2O_3/TiO_2 ratios (avg. 3.03 and 20.95, respectively), which are within the range of those of the PAAS (3.32 and 18.90, respectively), in agreement with geochemical maturity. This mature character is confirmed by the relatively high values of K_2O/Na_2O (avg. 5.81), with a probable increase of feldspars over plagioclases during sedimentary transport. The positive correlation among the Al_2O_3, Fe_2O_3 and K_2O contents suggests a moderate recycling character with the predominance of micas (muscovite and illite), which is also confirmed by an average index of compositional variability (ICV) value < 1 (Cox et al., 1995) (Table 1).

Relatively high CaO contents (avg. 2.69 wt.%), together with high LOI values (avg. 9.54 wt.%), rule out the use of the chemical index of alteration (CIA; Nesbitt and Young, 1982) to check the source weathering alteration. In turn, the plagioclase index of alteration (PIA; Fedo et al., 1995), with an average value of 72 (45–90) and similar to the PIA of the PAAS (79), suggests a plagioclase secondary conversion to clay minerals and supports an increased chemical maturity during post-depositional processes.

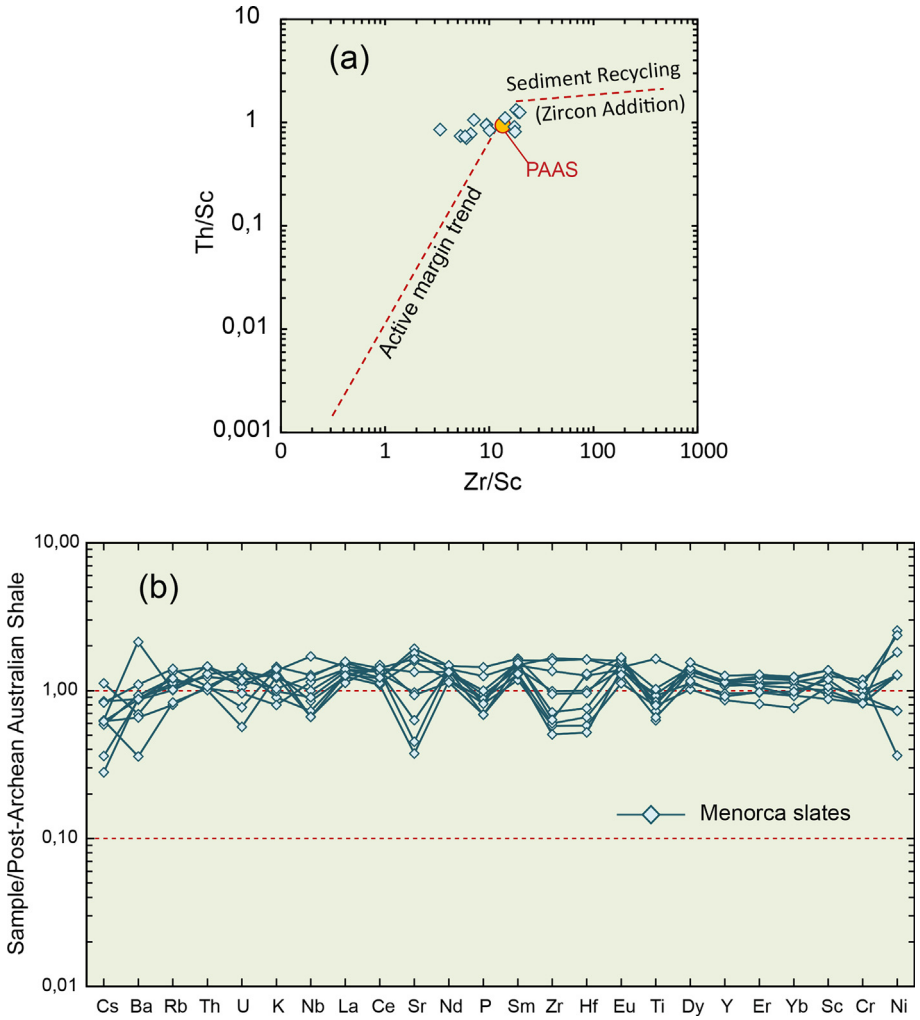

Fig. 7. (a) Th/Sc vs. Zr/Sc diagram (after McLennan et al., 1993). Menorca slates plot close to the PAAS and away from the typical compositional variations of active margin trends, suggesting some sedimentary recycling. (b) PAAS-normalised trace elements multi-variation diagrams (after Winchester and Max, 1989) of Devonian metasedimentary slates from Menorca. PAAS composition based on Taylor and McLennan (1985). Distant source areas and/or a constant extension of the sedimentary basin from Early Devonian to Carboniferous would explain the recycling features of these metasedimentary rocks.

The relatively higher average contents of some LILE elements (e.g. K, Cs, Ba, and Rb) compared to the PAAS confirmed this conclusion. Additionally, the Rb/Sr values of Menorcan slates point to a certain grade of post-depositional alteration. The majority of the samples present higher values than 0.5 (0.33–2.40; avg. 0.99), indicating a Sr redistribution in post-depositional processes (McLennan et al., 1993). The maturity and moderate recycling features of the Menorcan slates suggest a relatively long transport. The Devonian sedimentary basin would therefore be located far from the source areas, which involves a significant grade of sedimentary maturity with homogenous geochemical contents of major and trace elements. The Th/Sc (avg. 0.95) and Zr/Sc (avg. 11.28) ratios, similar to those of the PAAS (0.91 and 13.13, respectively), support some recycling in the sedimentary processes, with no Zr enrichment, which is frequent in highly recycled sedimentary rocks (Fig. 7a). The selected major and trace elements normalised to the PAAS from the Menorca slates display homogeneous patterns close to the normalisation values (Fig. 7b). This average composition being similar to that of the standard shale, with no evident LILE depletion, together with slightly negative Sr- and Ti-anomalies, support the idea of a significant influence of the sedimentary transport. Distant source areas and/or a constant extension of the sedimentary basin from the Early Devonian to the Carboniferous would explain the recycling features of these metasedimentary rocks.

Except for sample Nd-14, the bulk REE abundances in the Menorca slates are above those of the PAAS and show similar patterns (Fig. 8a, Table 1). These chondrite-normalised patterns exhibit high LREE fractionation (avg. La_N/Yb_N = 12.04), a slightly negative Eu- anomaly (avg. 0.67), and almost flat HREE patterns (avg. Gd_N/Yb_N = 1.72). All these features suggest a common felsic igneous source with an upper continental crust affinity (Bhatia, 1985; McLennan, 1989). This provenance is also confirmed by Al_2O_3/TiO_2 values similar to those of the PAAS (20.95 and 18.90, respectively) and very low Cr/V values (avg. 0.71) (Fig. 8b), which rules out a mafic/ultramafic provenance. High La (avg. 51 ppm) and Th (avg. 17 ppm) contents, above those of the PAAS (38.0 and 14.6 ppm, respectively), and La/Sc (avg. 2.88), Sc/Th (avg. 1.09), and Cr/Th (avg. 6.52) ratios similar to those of the PAAS (2.38, 1.10, and 7.53, respectively) also account for a felsic igneous affinity (Fig. 8c) (Cox et al., 1995; Cullers, 2002; McLennan et al., 2006).

3.2.2. Sr-Nd isotopic geochemistry

The Sm-Nd isotope information is given in Table 2 and Fig. 9, which show no large variation in the whole group of Menorca metasedimentary rocks. A Middle Devonian age of 390 Ma has been selected as a reference for Nd-isotope calculations. A relatively narrow range of variation observed in the initial $^{143}Nd/^{144}Nd$ ratios supports a similar source for the Menorca slates (0.51165–

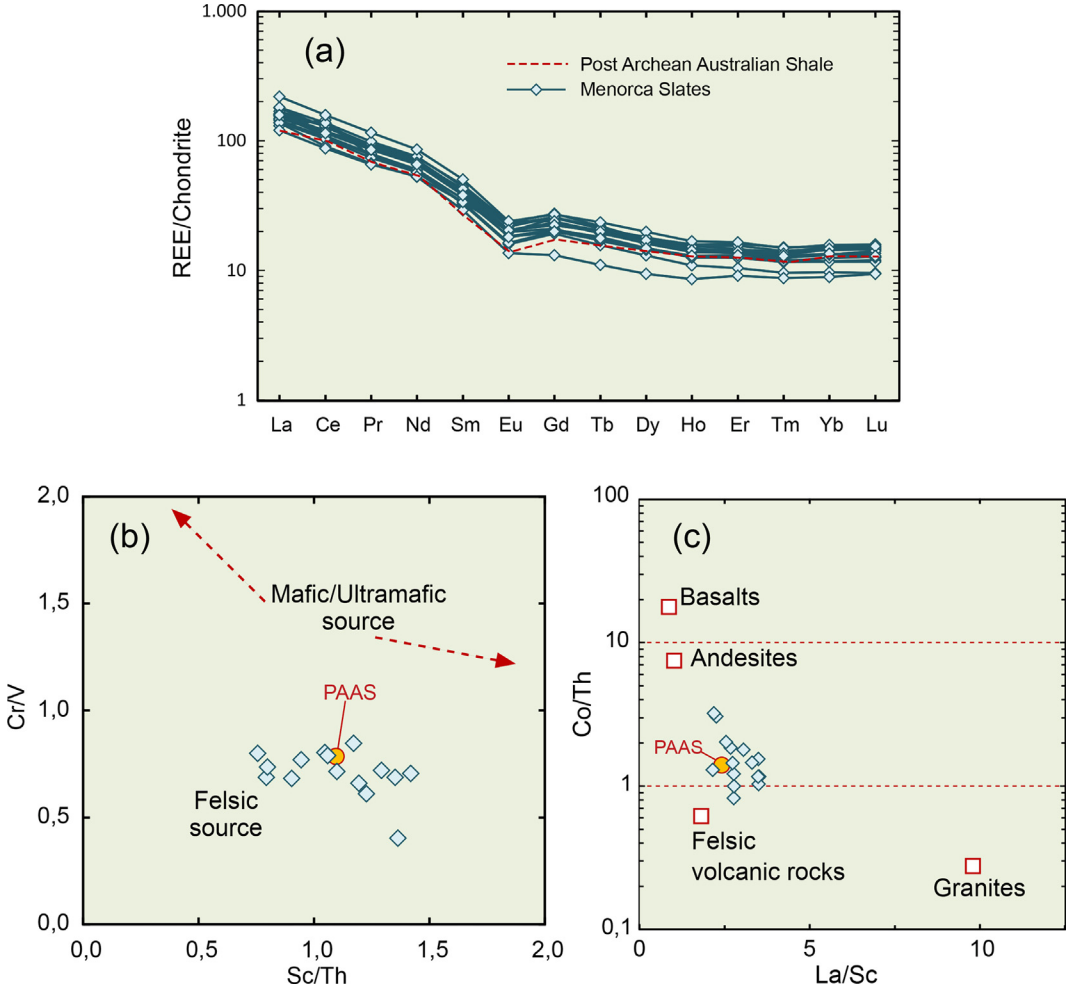

Fig. 8. (a) Chondrite normalised rare earth element patterns of metasedimentary rocks from Menorca. Normalising values are from Nakamura (1974). The dotted line corresponds to the PAAS (after Taylor and McLennan, 1985). (b) Cr/V vs. Sc/Th diagram; it shows a significant affinity of the metasedimentary rocks for a felsic source, far from mafic/ultramafic provenances. (c) Co/Th vs. La/Sc diagram for provenance discrimination of siliciclastic rocks (average compositions of igneous rocks from Condie, 1993). All of these features suggest a common felsic igneous source with an upper continental crust affinity.

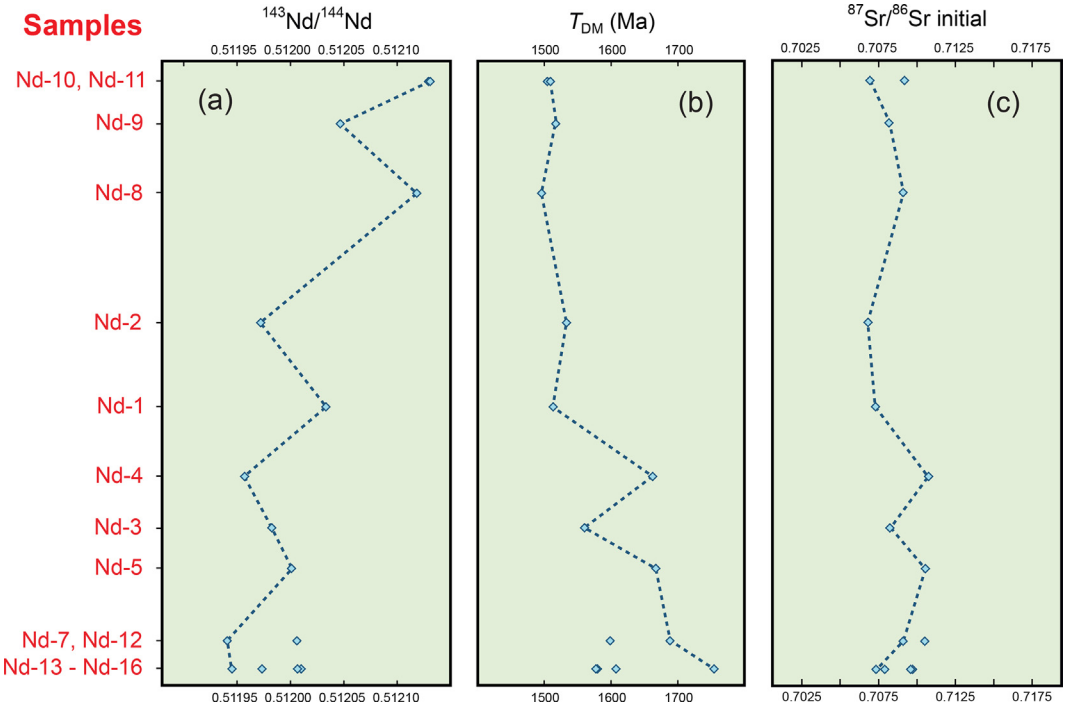

Fig. 9. Isotopic ratios in metapelites from Menorcan Devonian sequence. Bottom to top variations. (a) $^{143}Nd/^{144}Nd$ ratios. (b) T_{DM} plot showing variation of Nd model ages. (c) $^{87}Sr/^{86}Sr$ initial ratios. Explanation in details in the text.

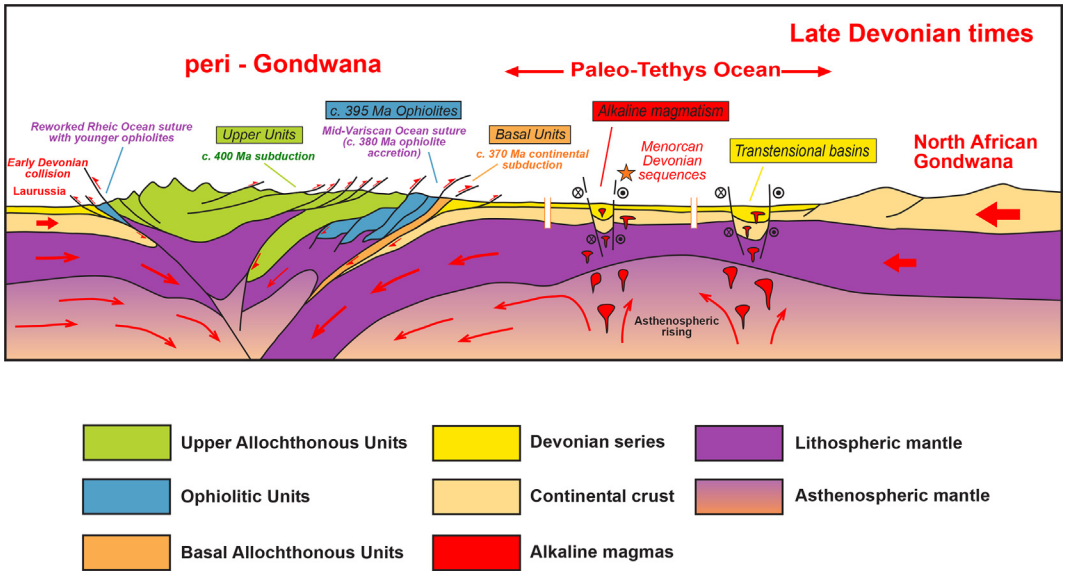

Fig. 10. Idealised section showing main units of the Variscan orogenic wedge and their structural organisation in Late Devonian times. The Devonian sequences furthest from the convergence zone were deposited on the *peri*-Gondwanan shelf in a context of dextral convergence and asthenospheric rising that generated deep mantle partial melting and alkaline magmatism. Based on Arenas et al. (2016) and Díez Fernández et al. (2016).

0.51182). The $^{147}Sm/^{144}Nd$ ratios vary between 0.1074 and 0.1238, within the range defined for siliciclastic rocks with a felsic crustal provenance (0.09–0.12; Sun et al., 1995). Ratios well > 0.08 rule out possible Sm fractionation in crustal processes (Bea et al., 2023) and as they are always < 0.165 they allow a reliable Nd model age calculation (Stern, 2002). No large variations are observed in $_{Nd(0)}$ (−13.6 to −9.9) or $_{Nd(390)}$, with values ranging from −9.5 to −6.2 (Table 2). However, we observe a marked trend in the analysed $^{143}Nd/^{144}Nd$ isotope ratios, from lower values of the samples collected at the base of the stratigraphic column (minimum value in Nd-12; 0.511941) to higher isotope ratios at the top (maximum value in Nd-11; 0.512131) (Fig. 9a). Nd model ages were calculated following the model proposed by DePaolo (1981), with values defining a narrow range between 1496 Ma and 1754 Ma (Late Paleoproterozoic–Early Mesoproterozoic; Fig. 9b). The tendency indicated above is also evident in the distribution of the T_{DM} values, which are progressively lower towards the top of the stratigraphic column (Table 2; Fig. 9b).

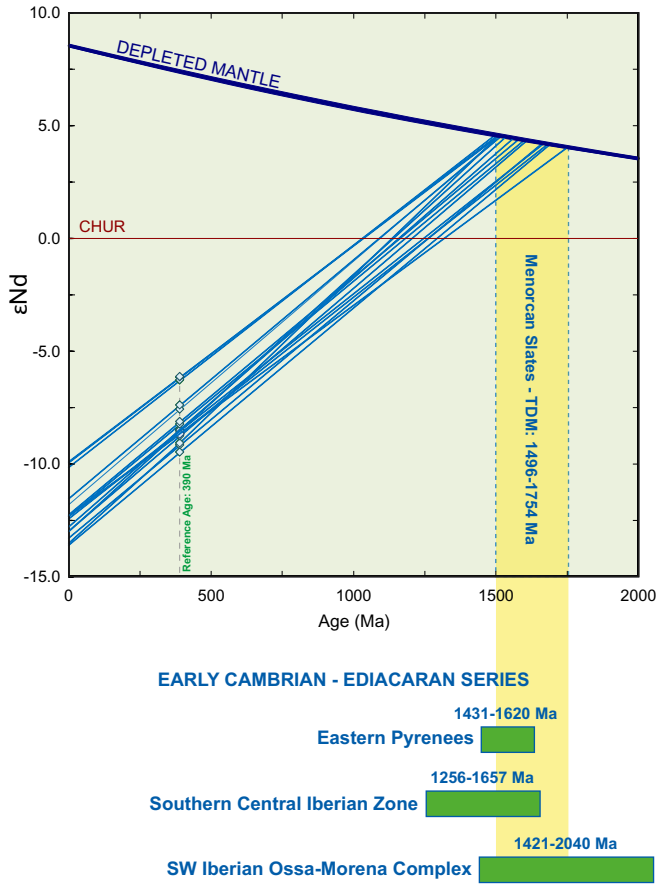

Fig. 11. T_{DM} vs. age (Ma) of Devonian metapelites from Menorca. A reference age of 390 Ma has been used for ε_{Nd} calculations. Devonian T_{DM} age range (1496–1754 Ma) is compared with model ages ranges characteristic of Ediacaran–Early Cambrian sequences from SW Iberian Ossa Morena Complex (Rojo-Pérez et al., 2019, 2021), Southern Central Iberian Zone (Fuenlabrada et al., 2016, 2020) and Eastern Pyrenees (Rojo-Pérez et al., 2023). Model ages calculated after DePaolo (1981).

The Sr isotope composition of Menorcan metasedimentary rocks shows a relatively large variation, with $^{87}Sr/^{86}Sr$ ratios ranging from 0.715087 to 0.745513 (Table 3), this is also visible in the wide range displayed by the $^{87}Rb/^{86}Sr$ isotope ratios (0.9617–6.9695). A highly negative correlation of the Sr content and $^{87}Sr/^{86}$-Sr ratios, while the Rb content remains relatively homogeneous (Table 1), together with the evident variability of the $^{87}Sr/^{86}Sr$ ratios, agrees with a differentiated isotopic evolution from highly homogeneous values of the $^{87}Sr/^{86}Sr$ initial ratio (0.706809–0.710753; Fig. 9c). The low range of the initial Sr isotope compositions suggests that the Menorcan Devonian slates were sourced from areas with a marked continental crustal affinity, with values within the range between 0.7025 and 0.730 (White, 2013).

4. Discussion

4.1. The Paleozoic basement of Menorca in the Variscan orogen

The pre-orogenic Devonian sequence of Menorca was deposited somewhere on the North African margin of Gondwana. After the Variscan Orogeny, this region was located on the eastern limb of the Ibero-Armorican arc (Fig. 1). Assuming that the regional tectonic transport of the first contractional Variscan structures was directed towards the foreland located towards Gondwana, the W-directed tectonic transport of Variscan thrusts in Menorca supports a late rotation of Menorcan units associated with the generation of the Ibero-Armorican arc. The initial location of the Balearic Islands at the end of Variscan deformation is subject to some uncertainty, due to the important dynamics associated with the post-Variscan opening of the Mediterranean Sea (Alpine-Tethys Ocean; Stampfli and Borel, 2002). However, a location close to the current one, next to the eastern margin of Iberia is generally accepted (Edel et al., 2014; Pellen et al., 2016). This location is perpendicular to the prolongation of the geotectonic zones of the Iberian Massif towards the eastern limb of the Ibero-Armorican arc (Fig. 1), and it indicates that the Paleozoic units of Menorca can be correlated with equivalent units in the Central Iberian Zone. A thick Devonian sequence has been described in the southern part of the Central Iberian Zone in the Almadén syncline. This sequence is also characterised by the presence of an alkaline volcanism (Sainz de Baranda and Lunar Hernández, 1989). Also in the Central Iberian Zone, another Devonian sequence with associated volcanism has been described in the Sierra del Castillo region (Gutiérrez Alonso et al., 2008). Considering the similarities of the Devonian sequences, the location of Menorca in the Ibero-Armorican arc (Fig. 1), and the existence of alkaline magmatism in Menorca, the correlation of these sequences is plausible.

The precise age of the Variscan deformation affecting the Menorcan pre-orogenic Devonian sequence is unknown, although it occurred in Early Carboniferous times. However, the characteristics of the Menorca-type Devonian basins on the Gondwana margin in fact can be determined, once the units of the Ibero-Armorican arc are restored to their original position and the Variscan orogenic wedge is reconstructed (Fig. 10). These basins were formed in a context of dextral convergence between Laurussia and Gondwana, in a forward position in relation to the advancing deformation and in an active setting with asthenospheric rising and associated alkaline magmatism (Fig. 10). They probably were rather narrow basins (Card and Mortenari, 2023), with a high dynamic influence, housing sequences thicker than the more common shallower *peri*-Gondwanan Devonian sequences (Fig. 10). The collision between Laurussia and Gondwana developed several subduction zones with different polarities further north and occurred after the closure of the Rheic Ocean and other minor oceanic domains (Nance et al., 2010; Arenas et al., 2016; Díez Fernández et al., 2016). This orogenic evolution can be recognised throughout the Variscan Orogen, from the Iberian Massif to the Bohemian Massif, where a succession of correlatable allochthonous and autochthonous terranes has been described (Martínez Catalán et al., 2020; Schulmann et al., 2022). Variscan deformation affected the section of the *peri*-Gondwanan shelf that contained the Menorcan Devonian sequence throughout the Early Carboniferous. During this deformation, the thick Kulm Facies Carboniferous unit that characterises the eastern sector of the island was deposited. After the Ibero-Armorican arc is restores, these Carboniferous units occupy a more hinterland position in the orogen. Kulm Facies Carboniferous sequences have in fact been found in the Iberian Massif in the western limb of the arc, in a similar position.

4.2. Provenance of the Devonian sequence of Menorca

The major and trace element contents of the Menorca Devonian metapelites are characteristic of siliciclastic rocks with moderate recycling and rather long transport. Their source areas were distant and showed the predominance of upper crustal felsic rocks. Therefore, they were domains of upper continental crust located in North African Gondwana. To explore the provenance of the Menorcan Devonian sequence, the two investigated isotopic systems (Rb-Sr and Sm-Nd) can be used. The initial $^{87}Sr/^{86}Sr$ ratio does not register a significant variation throughout the Devonian sequence (Fig. 9c), which could at first indicate little variation in source areas during the Devonian. However, the high chemical mobility of this

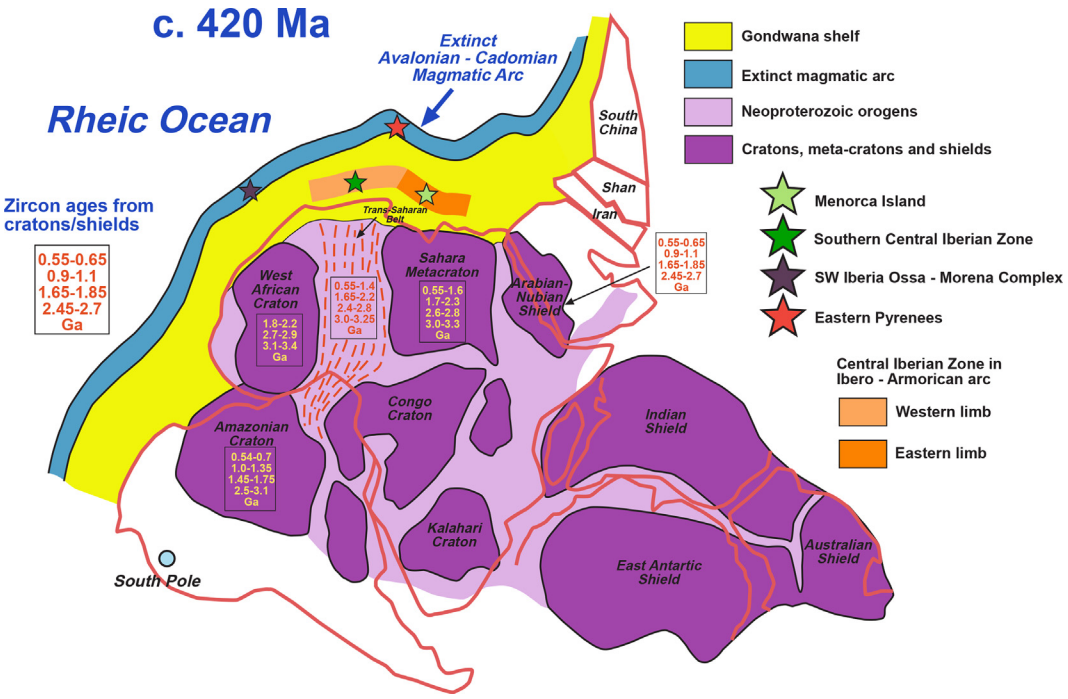

Fig. 12. Gondwana reconstruction at c. 420 Ma showing inferred location of Devonian Menorcan sequences. Location at that time of different regions from Variscan Iberia are also shown. Reported zircon ages from cratons after Avigad et al. (2012), Morag et al. (2012), Linnemann et al. (2014) and Padel et al. (2022). See text for explanations.

system can favour homogenisation during sedimentary transport and recycling, which are both reflected in the chemistry of the rocks, and limits the application of this isotopic system for provenance analysis.

However, the Sm-Nd system provides significant provenance information. Fig. 11 shows an ε_{Nd}-age (Ma) diagram with a representation of the T_{DM} range recorded by the metapelites. At present, there is no consistent database with the T_{DM} values of Devonian siliciclastic units in the Variscan Orogen or in North Africa, so a direct comparison of the data from Menorca with data from other regions is not possible. However, there is a representative database of Nd model ages of the Ediacaran and Early Cambrian units of the Iberian Massif (Fuenlabrada et al., 2016, 2020; Rojo Pérez et al., 2019, 2021, 2023), a representation of which is shown in Fig. 11. Older T_{DM} ranges indicate a provenance from the West Africa Craton or its peripheral domain, while younger T_{DM} ranges reflect a provenance from more easterly North African regions in the Sahara Metacraton or Arabian-Nubian Shield. This interpretation is based on the lithostratigraphy of the North African terranes, characterised by decreasing ages from the West Africa Craton and its periphery to the Arabian-Nubian Shield (Abalos et al., 2012; Brahimi et al., 2018). These data are in line with the existence of two differentiated *peri*-Gondwanan shelves in North Africa (Stephan et al., 2019), whose siliciclastic sequences show different average T_{DM} values (Fuenlabrada et al., 2023). The younger character of the North African continental crust towards the easternmost regions is also supported by the higher content of Mesoproterozoic and Pan-African detrital zircons recorded in siliciclastic sequences, with an opposite decrease in the Paleo-Proterozoic and Archean populations characteristic of western North Africa (Díez Fernández et al., 2010; Fernández Suárez et al., 2014; Shaw et al., 2014).

Based on the Nd isotopic contents and the T_{DM} values (1496–1754 Ma), and despite the different ages of the units considered, the absence of Nd model ages older than 1754 Ma in the Devonian sequence of Menorca should exclude a direct provenance from the erosion of the WAC or its more peripheral domains. These T_{DM} values are more consistent with a more uncertain provenance, but they are more closely related to more easterly source areas, located in either the Trans-Saharan Belt or the Sahara Meta-Craton (Fig. 12). These results are also compatible with data provided by detrital zircons from the sequence from northern Menorca, although in this case an even more easterly North African provenance has been suggested (Cristóbal et al., 2023).

4.3. Variscan convergence and dextral motion

The Nd isotope geochemistry of the Menorcan Devonian sequence shows a significant rejuvenation of T_{DM} values from bottom to top, from c. 1700 Ma to c. 1500 Ma (average values). This evolution over such a short period of time is not consistent with a stable source. It requires a significant isotopic rejuvenation of the source, either because of an increasing contribution of juvenile material or due to the variation of the source area. The first case is highly unlikely, since the North African domain to the east of the Trans-Saharan Belt was stable during Devonian times. The second situation is more compatible with the dynamics developed during the Variscan Orogeny. The convergence between Laurussia and Gondwana had an important dextral component (Díez Fernández et al., 2012; Arenas et al., 2014; Martínez Catalán et al., 2021). The dextral rotation of Gondwana during the Devonian, coeval with the Variscan deformation, may explain the progressive approximation of more easterly African domains to the *peri*-Gondwanan sectors located immediately further south of the Variscan orogenic wedge (Fig. 12). A similar evolution has been proposed to explain the variation in Nd isotopic contents observed in the Ediacaran sequences from the Iberian Massif (Rojo-Pérez et al., 2023). Dextral convergence could also favour the development of narrow Devonian basins with thick sedimentary sequences, as well as an asthenospheric rising and the generation of alkaline magmatism.

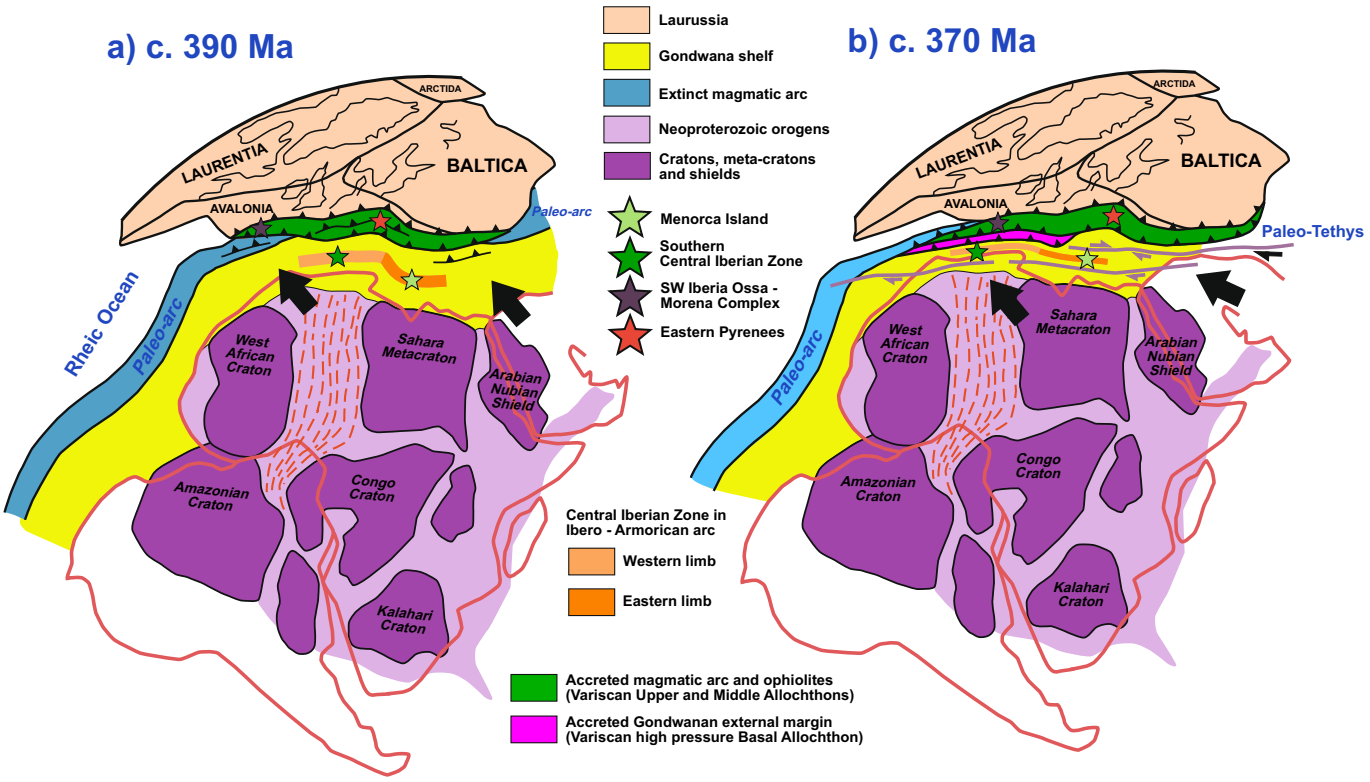

Fig. 13. Sketch showing the dextral rotation of Gondwana at the onset of the Variscan deformation at (a) 390 Ma and (b) 370 Ma. The westward translation of the Central Iberian Zone, and the approximation of progressively more eastern sectors of Gondwanan regions to the Menorcan Devonian basin, favored the rejuvenation of Nd model ages. See text for explanations.

4.4. The western frontiers of the Paleo-Tethys Ocean

The development of significant Devonian dynamics further south of the Variscan Orogen has been repeatedly suggested. Stampfli and Borel (2002) and Stampfli et al. (2013) consider this *peri*-Gondwanan domain experienced rifting that favoured the opening of the Paleo-Tethys Ocean. Ophiolites that demonstrate the existence of this ocean have not been found to date in any part of the European basement, although the development of a volcanic arc linked to the closure of this ocean in Late Carboniferous–Early Permian times has been considered (Pereira et al., 2015). In any case, the data provided in this work indicate that the arrival of siliciclastic material from North Africa to the *peri*-Gondwanan Devonian basins was apparently not interrupted during this period. The T_{DM} values obtained for the Devonian sequence of Menorca record a continuous evolution but do not show an abrupt change that can be interpreted as an interruption of the arrival of siliciclastic material from the south (North Africa). These data must be interpreted in the sense that there was not a large oceanic domain during Devonian times to the south of Iberia able to block the arrival of detrital material from North Africa. A large tract of the Paleo-Tethys Ocean would therefore not have existed during the Devonian south of Iberia. This ocean must therefore have had limited extent in this period towards the westernmost sectors. The Devonian *peri*-Gondwanan shelf was apparently continuous around Iberia (Fig. 13). This platform was progressively affected by Variscan deformation advancing from north to south and incorporated into the Variscan orogenic wedge with the same vergence.

The possible opening of the Paleo-Tethys Ocean south of Iberia during the Carboniferous has not been directly investigated in this work. However, the c. 3000-m-thick Carboniferous sequence on Menorca Island is of Kulm Facies and *syn*-orogenic character (Rosell et al., 1987a, 1987b). The age of the Kulm-type Carboniferous unit is considered Mississippian (c. 359–318 Ma; Aretz, 2016). These characteristics suggest that the sequence was deposited at an advanced stage of the Variscan Orogeny, that is, the convergence between Gondwana and Laurussia. This scenario of intracontinental deformation is not compatible with the contemporary opening of a broad oceanic domain. It is therefore also unlikely that the Paleo-Tethys Ocean extended south of Iberia during the Mississippian. Therefore, current data indicate that the Paleo-Tethys Ocean did not have continuous E–W extension north of Gondwana. Its domains, in the sense of a true ocean with an oceanic lithosphere generated at a mid-ocean ridge, must therefore have ended up in a position significantly further east than the domain occupied by Iberia.

5. Conclusions

The stratigraphic, magmatic and deformation characteristics of the Devonian sequences from northern Menorca suggest a possible correlation with southern sectors of the Central Iberian Zone on the western limb of the Iberian-Armorican arc. The Variscan deformation of these sequences shows an apparent vergence towards the west, which is compatible with its current position on the eastern side of the arc. The Devonian metapelites have major and trace element contents that indicate equivalence with mature, moderately recycled siliciclastic rocks that have undergone long transport. The Nd isotopic composition indicates a provenance from source areas located in North African Gondwana in sectors further east of the West African Craton, probably belonging to the Trans-Saharan Belt or the Sahara Meta-Craton. The T_{DM} values of these metapelitic rocks show the gradual variation from bottom to top of the Devonian unit, from c. 1700 Ma to c. 1500 Ma (average values). This variation is interpreted in relation to the rotation of Gondwana

during the Variscan convergence with Laurussia, which had a dextral character and could approximate eastern North African domains with younger isotopic signatures (T_{DM}). The gradual variation during the Devonian of the T_{DM} values rules out the existence of any break in the *peri*-Gondwanan shelf of this age to the south of Iberia. This data restricts the development of an extensive Paleo-Tethys Ocean to *peri*-Gondwanan domains located considerably further east than Iberia.

CRediT authorship contribution statement

Ricardo Arenas: Conceptualization, Funding acquisition, Writing – original draft, Investigation, Writing – review & editing. **José M. Fuenlabrada:** Formal analysis, Investigation, Methodology, Software, Writing – original draft. **Cristian Timoner:** Investigation, Supervision. **Rubén Díez Fernández:** Validation, Visualization. **Esther Rojo-Pérez:** Data curation, Resources.

Acknowledgements

Insightful revisions of the manuscript by Eirini Poulaki, Salvatore Critelli and two other anonymous reviewers is kindly acknowledged. We also appreciate the editorial handling of Associate Editor Dr. Stijn Glorie, the Editorial Advisor of Prof. M. Santosh and the opportunity given by China University of Geosciences Beijing to publish this work in Geoscience Frontiers. Financial support has been provided by the Spanish projects PID2020-112489 GB-C21 and PID2020-112489 GB-C22 funded by MCIN/AEI.

References

Abalos, B., Gil Ibarguchi, I., Sánchez-Lorda, M.E., Paquette, J.L., 2012. African/Amazonian proterozoic correlations of Iberia: a detrital zircon U-Pb study of early Cambrian conglomerates from the Sierra de la Demanda (Northern Spain). Tectonics 31, TC3003.

Albert, R., Arenas, R., Gerdes, A., Sánchez Martínez, S., Fernández-Suárez, J., Fuenlabrada, J.M., 2015a. Provenance of the Variscan Upper Allochthon (Cabo Ortegal Complex, NW Iberian Massif). Gondw. Res. 28, 1434–1448.

Albert, R., Arenas, R., Gerdes, A., Sánchez Martínez, S., Marko, L., 2015b. Provenance of the HP-HT subducted margin in the Variscan belt (Cabo Ortegal Complex, NW Iberian Massif). J. Metam. Geol. 33, 959–979.

Arenas, R., Díez Fernández, R., Sánchez Martínez, S., Gerdes, A., Fernández-Suárez, J., Albert, R., 2014. Two-stage collision: Exploring the birth of Pangea in the Variscan terranes. Gondw. Res. 25, 756–763.

Arenas, R., Sánchez Martínez, S., Díez Fernández, R., Gerdes, A., Abati, J., Fernández-Suárez, J., Andonaegui, P., González Cuadra, P., López Carmona, A., Albert, R., Fuenlabrada, J.M., Rubio Pascual, F.J., 2016. Allochthonous terranes involved in the Variscan suture of NW Iberia: A review of their origin and tectonothermal evolution. Earth Sci. Rev. 161, 140–178.

Arenas, R., Novo-Fernández, I., García-Casco, A., Díez Fernández, R., Fuenlabrada, J. M., Pereira, M.F., Abati, J., Sánchez Martínez, S., Rubio Pascual, F.J., 2021. A unique blueschist facies metapelite with Mg-rich chloritoid from the Badajoz-Córdoba Unit (SW Iberian Massif): Correlation of Late Devonian high-pressure belts along the Variscan Orogen. Int. Geol. Rev. 63, 1634–1657.

Aretz, M., 2016. The Kulm Facies of the Montagne Noire (Mississipian, southern France). Geol. Belg. 19, 69–80.

Avigad, D., Gerdes, A., Morag, N., Bechstädt, T., 2012. Coupled U-Pb-Hf of detrital zircons of Cambrian sandstones from Morocco and Sardinia: Implications for provenance and Precambrian crustal evolution of North Africa. Gondw. Res. 21, 690–703.

Avigad, D., Avishai, A., Gerdes, A., Schmitt, A.K., 2022. Crustal evolution of Western Europe: Constraints from detrital zircon U-Pb-Hf-O isotopes. Gondw. Res. 106, 379–396.

Bea, F., Montero, P., Barcos, L., Cambeses, A., Molina, J.F., Morales, I., 2023. Understanding Nd model ages of granite rocks: The effects of the $^{147}Sm/^{144}Nd$ variability during partial melting and crystallization. Lithos 436–437, 106940.

Bhatia, M.R., 1985. Rare earth element geochemistry of Australian Paleozoic graywackes and mudrocks: Provenance and tectonic control. Sed. Geol. 45, 97–113.

Bourrouilh, R., 1983. Estratigrafía, sedimentología y tectónica de la isla de Menorca y del Noreste de Mallorca (Baleares). La terminación nororiental de las Cordilleras béticas en el Mediterraneo occidental. Memorias Del Instituto Geológico y Minero De España 99, 672 pp (in Spanish).

Brahimi, S., Liégeois, J.P., Ghienne, J.F., Munschy, M., Bourmatte, A., 2018. The Tuareg shield terranes revisited and extended towards the northern Gondwana margin: Magnetic and gravimetric constraints. Earth Sci. Rev. 185, 572–599.

Card, C.J., Montenari, M., 2023. Comparative geochemistry of Early Carboniferous marine red beds (MRBs) and their significance for deep time paleoceanographic reconstructions. Sed. Geol. 444, 106313.

Caro, G., Bourdon, B., 2010. Non-chondritic Sm/Nd ratio in the terrestrial planets: consequences for the geochemical evolution of the mantle–crust system. Geochim. Cosmochim. Acta 74, 3333–3349.

Condie, K.C., 1993. Chemical composition and evolution of the upper continental crust: Contrasting results from surface samples and shales. Chem. Geol. 104, 1–37.

Costamagna, L., Criniti, S., 2024. Interpreting siliciclastic sedimentation in the upper Paleozoic Mulargia-Escalaplano Basin (Sardinia, Italy): Influence of tectonics on provenance. J. Palaeogeogr. 13, 18–34.

Cox, R., Lowe, D.R., Cullers, R.L., 1995. The influence of sediment recycling and basement composition on evolution of mudrock chemistry in the southwestern United States. Geochim. Cosmochim. Acta 59, 2919–2940.

Criniti, S., 2023. Detrital modes of buried Permian sandstones of the Puglia 1 well (Puglia Region, Southern Italy). Rendiconti Online Società Geologica Italiana 59, 119–124 (in Spanish).

Criniti, S., Martín-Martín, M., Martín-Algarra, A., 2023. New constraints for the western Paleotethys paleogeography-paleotectonics derived from detrital signatures: Malaguide Carboniferous Culm Cycle (Betic Cordillera, S Spain). Sed. Geol. 458, 1–27.

Cristóbal, L.S., Booth-Rea, G., Garrido, C.J., 2023. Análisis y comparación de circones detríticos de Menorca y del Complejo Maláguide: implicaciones para el origen del Dominio de Alboran. Macla (Revista de la Sociedad Española de Mineralogía). Macla 27, 33–34 (in Spanish).

Critelli, S., 2018. Provenance of Mesozoic to Cenozoic circum-Mediterranean sandstones in relation to tectonic setting. Earth Sci. Rev. 185, 624–648.

Critelli, S., Perri, F., Arribas, J., Herrero, M.J., 2018. Sandstone detrital modes and diagenetic evolution of Mesozoic continental redbeds from western-central circum-Mediterranean orogenic belts. In: Ingersoll, R.V., Lawton, T.F., Graham, S. (Eds.), Tectonics, Sedimentary Basins and Provenance: A Celebration of William R. Dickinson's Career. Geological Society of America Special Paper 540, pp. 119-132.

Critelli, S., Martín-Martín, M., 2022. Provenance, paleogeographic and paleotectonic interpretations of Oligocene-Lower Miocene sandstones of the western-central Mediterranean region: A review. Journal of Asian Earth Sciences X 8, 100124.

Critelli, S., Martín-Martín, M., 2024. History of western Tethys Ocean and the birth of the circum-Mediterranean orogeny as reflected by source-to-sink relations. Int. Geol. Rev. 66, 505–515.

Critelli, S., Reed, W.E., 1999. Provenance and stratigraphy of the Devonian (Old Red Sandstone) and Carboniferous sandstones of Spitsbergen, Svalbard. Eur. J. Mineral. 11, 149–166.

Cullers, R.L., 2002. Implications of elemental concentrations for provenance, redox conditions, and metamorphic studies of shales and limestones near Pueblo, CO, USA. Chem. Geol. 191, 305–327.

DePaolo, D.J., 1981. A neodymium and strontium isotopic study of the Mesozoic calc-alkaline granitic batholiths of the Sierra Nevada and Peninsular Ranges, California. J. Geophys. Res. 86, 10470–10488.

Díez Fernández, R., Martínez Catalán, J.R., Gerdes, A., Abati, J., Arenas, R., Fernández-Suárez, J., 2010. U-Pb ages of detrital zircons from the basal allochthonous units of NW Iberia: Provenance and paleoposition on the northern margin of Gondwana during the Neoproterozoic and Paleozoic. Gondw. Res. 18, 385–399.

Díez Fernández, R., Martínez Catalán, J.R., Arenas, R., Abati, J., 2012. The onset of the assembly of Pangaea in NW Iberia: Constraints on the kinematics of continental subduction. Gondw. Res. 22, 20–25.

Díez Fernández, R., Arenas, R., Pereira, M.F., Sánchez-Martínez, S., Albert, R., Martín Parra, L.M., Rubio Pascual, F.J., Matas, J., 2016. Tectonic evolution of Variscan Iberia: Gondwana-Laurussia collision revisited. Earth Sci. Rev. 162, 269–292.

Edel, J.B., Casini, L., Oggiano, G., Rossi, P., Schulmann, K., 2014. Early Permian clockwise 90° rotation of the Maures-Estérel-Corsica-Sardinia block confirmed by new palaeomagnetic data and followed by a Triassic 60° clockwise rotation. In: Schulmann, K., Martínez Catalán, J.R., Lardeaux, J.M., Janousek, V., Oggiano, G. (Eds.), The Variscan Orogeny: Extent, timescale and the formation of the European Crust. Geological Society, London, Special Publications 405, pp. 333–361.

Fedo, C.M., Nesbitt, H.W., Young, G.M., 1995. Unravelling the effects of potassium metasomatism in sedimentary rocks and paleosols, with implications for paleoweathering conditions and provenance. Geology 23, 921–924.

Fernández-Suárez, J., Gutiérrez-Alonso, G., Pastor-Galán, D., Hofmann, M., Murphy, J.B., Linnemann, U., 2014. The Ediacaran-Early Cambrian detrital zircon record of NW Iberia: possible sources and paleogeographic constraints. Int. J. Earth Sci. 103, 1335–1357.

Franke, W., Cocks, L.R.M., Torsvik, T.H., 2017. The Palaeozoic Variscan oceans revisited. Gondw. Res. 48, 257–284.

Fuenlabrada, J.M., 2023. High-precision Sr and Nd isotope characterization of BHVO-2 reference material by thermal ionization mass spectrometry. Rapid Communications in Mass Spectrometry 37, e9632.

Fuenlabrada, J.M., Pieren, A.P., Díez Fernández, R., Sánchez Martínez, S., Arenas, R., 2016. Geochemistry of the Ediacaran-Early Cambrian transition in Central Iberia: Tectonic setting and isotopic sources. Tectonophysics 681, 15–30.

Fuenlabrada, J.M., Arenas, R., Sánchez Martínez, S., Díez Fernández, R., Pieren, A.P., Pereira, M.F., Chichorro, M., Silva, J.B., 2020. Geochemical and isotopic (Sm-Nd) provenance of Ediacaran-Cambrian metasedimentary series from the Iberian Massif. Paleoreconstruction of the North Gondwana margin. Earth Sci. Rev. 201, 103079.

Fuenlabrada, J.M., Arenas, R., Pereira, M.F., Rojo-Pérez, E., Sánchez Martínez, S., Díez Fernández, R., 2023. Variability in the sources of North Gondwana Cadomian basins tracked by Nd isotopic systematics (Iberian Massif). Precambr. Res. 397, 107185.

García, R., Brell, J.M., Aparicio, A., 1992. El metamorfismo del Paleozoico de la isla de Menorca (Islas Baleares). Bol. Geol. Miner. 103, 564–569. in Spanish.

Gutiérrez Alonso, G., Murphy, J.B., Fernández-Suárez, J., Hamilton, M.A., 2008. Rifting along the northern Gondwana margin and the evolution of the Rheic Ocean: A Devonian age for the El Castillo volcanic rocks (Salamanca, Central Iberian Zone). Tectonophysics 461, 157–165.

Hatcher, R.D., 2010. The Appalachian orogen: A brief summary. Memoir of the Geological Society of America 206, 1–19.

Jacobsen, S.B., Wasserburg, G.J., 1980. Sm-Nd isotopic evolution of chondrites. Earth Planetary Science Letters 50, 139–155.

Kairouani, H., Zaghloul, M.N., Abbassi, A., Micheletti, F., Fornelli, A., El Mourabet, M., Piccoli, F., Criniti, S., Critelli, S., 2023. Provenance and source-to-sink of lower-middle Jurassic sediments from hinterland mounts to NW-Gondwana hyper-extended passive margin (Prerif sub-domain, External Rif, Morocco): First evidence from sedimentary petrology and detrital zircon geochronology. Mar. Pet. Geol. 157, 106492.

Kroner, U., Romer, R.L., 2013. Two plates - Many subduction zones: The Variscan Orogeny reconsidered. Gondw. Res. 24, 298–329.

Linnemann, U., Gerdes, A., Hofmann, M., Marko, L., 2014. The Cadomian Orogen: Neoproterozoic to Early Cambrian crustal growth and orogenic zoning along the periphery of the West African Craton. Constraints from U-Pb zircon ages and Hf isotopes (Schwarzburg Antiform, Germany). Precambr. Res. 244, 236–278.

Linnemann, U., Romer, R., 2002. The Cadomian Orogeny in Saxo-Thuringia, Germany: Geochemical and Nd–Sr–Pb isotopic characterization of marginal basins with constraints to geotectonic setting and provenance. Tectonophysics 352, 33–64.

Linnemann, U., Ouzegane, K., Drareni, A., Hofman, M., Becker, S., Gärtner, A., Sagawe, A., 2011. Sands of West Gondwana: An archive of secular magmatism and plate interactions — A case study from the Cambro-Ordovician section of the Tassili Ouan Ahaggar (Algerian Sahara) using U-Pb–LA-ICP-MS detrital zircon ages. Lithos 123, 188–203.

Lugmair, G.W., Marti, K., 1978. Lunar initial $^{143}Nd/^{144}Nd$: differential evolution of the lunar crust and mantle. Earth Planet. Scence. Letters 39, 349–357.

Martínez Catalán, J.R., Arenas, R., Abati, J., Sánchez Martínez, S., Díaz García, F., Fernández-Suárez, J., González Cuadra, P., Castiñeiras, P., Gómez Barreiro, J., Díez Montes, A., González Clavijo, E., Rubio Pascual, F.J., Andonaegui, P., Jeffries, T.E., Alcock, J.E., Díez Fernández, R., López Carmona, A., 2009. A rootless suture and the loss of the roots of a mountain chain: The Variscan belt of NW Iberia. C. r. Geosci. 341, 114–126.

Martínez Catalán, J.R., Collett, S., Schulmann, K., Aleksandrowski, P., Mazur, S., 2020. Correlation of allochthonous terranes and major tectonostratigraphic domains between NW Iberia and the Bohemian Massif, European Variscan belt. International Journal of Earth Sciences 109, 1105–1131.

Martínez Catalán, J.R., Schulman, K., Ghienne, J.-F., 2021. The Mid-Variscan Allochthon: Keys from correlation, partial retrodeformation and plate-tectonic reconstruction to unlock the geometry of a non-cylindrical belt. Earth Sci. Rev. 220, 103700.

Martinez, F.J., Dietsch, C., Aleinikoff, J., Cires, J., Arboleya, M.L., Reche, J., Gomez-Gras, D., 2016. Provenance, age, and tectonic evolution of Variscan flysch, southeastern France and northeastern Spain, based on zircon geochronology. Geological Society of America Bulletin 128, 842–859.

Matte, Ph., 1991. Accretionary history and crustal evolution of the Variscan belt in western Europe. Tectonophysics 196, 309–337.

McLennan, S.M., 1989. Rare earth elements in sedimentary rocks: Influence of provenance and sedimentary processes. Mineralogical Society of America, Reviews in Mineralogy 21, 169–200.

McLennan, S.M., Hemming, S.R., McDaniel, D.K., Hanson, G.N., 1993. Geochemical approaches to sedimentation, provenance and tectonics. In: Johnssons, M.J., Basu, A. (Eds.), Processes controlling the composition of clastic sediments. Geological Society of America. Special Paper 284, pp. 21-40.

McLennan, S.M., Taylor, S.R., Hemming, S.R., 2006. Composition, differentiation, and evolution of continental crust: Constrains from sedimentary rocks and heat flow. In: Brown, M., Rushmer, T. (Eds.), Evolution and Differentiation of the Continental Crust. Cambridge University Press, pp. 92–134.

Morag, N., Avigad, D., Gerdes, A., Harlavan, Y., 2012. 1000–580Ma crustal evolution in the northern Arabian-Nubian Shield revealed by U-Pb–Hf of detrital zircons from late Neoproterozoic sediments (Elat area, Israel). Precambr. Res. 208–211, 197–212.

Nakamura, N., 1974. Determination of REE, Ba, Fe, Mg, Na and K in carbonaceous and ordinary chondrites. Geochimica et Cosmochimica Acta 38, 757–775.

Nance, R.D., Gutiérrez-Alonso, G., Keppi, J.D., Linnemann, U., Murphy, J.B., Quesada, C., Strachan, R.A., Woodcock, N.H., 2010. Evolution of the Rheic Ocean. Gondw. Res. 17, 194–222.

Nesbitt, H.W., Young, G.M., 1982. Early Proterozoic climates and plate motions inferred from major element chemistry of lutites. Nature 299, 715–717.

Nier, A., 1938. Isotopic constitution of Sr, Ba, Bi, Tl and Hg. Phys. Rev. 54, 275–278.

O'Nions, R.K., Carter, S.R., Evensen, N.M., Hamilton, P.J., 1979. Geochemical and cosmochemical applications of Nd isotope analysis. Annu. Rev. Earth Planet. Sci. 7, 11–38.

Padel, M., Clausen, S., Poujol, M., Álvaro, J.J., 2022. Shifts in the Ediacaran to Lower Ordovician sedimentary zircon provenances of Northwest Gondwana: The Pyrenean files. Geol. Acta 20 (14), 1–18.

Pellen, R., Aslanian, D., Rabineau, M., Leroux, E., Gorini, C., Silenziano, C., Blanpied, C., Rubino, J.-L., 2016. The Minorca Basin: A buffer zone between the Valencia and Liguro-Provençal Basins (NW Mediterranean Sea). Terra Nova 28, 245–256.

Pereira, M.F., Solá, A.R., Chichorro, M., Lopes, L., Gerdes, A., Silva, J.B., 2012. North-Gondwana assembly, break up and paleogeography: U-Pb isotope evidence from detrital and igneous zircons of Ediacaran and Cambrian rocks of SW Iberia. Gondw. Res. 22, 866–881.

Pereira, M.F., Castro, A., Fernández, C., 2015. The inception of a Paleotethyan magmatic arc in Iberia. Geosci. Front. 6, 297–306.

Pereira, M.F., Gutiérrez Alonso, G., Murphy, J.B., Drost, K., Gama, C., Silva, J.B., 2017. Birth and demise of the Rheic Ocean magmatic arc(s): Combined U-Pb and Hf isotope analyses in detrital zircon from SW Iberia. Lithos 278–281, 383–399.

Rojo-Pérez, E., Arenas, R., Fuenlabrada, J.M., Sánchez Martínez, S., Martín Parra, L.M., Matas, J., Pieren, A.P., Díez Fernández, R., 2019. Contrasting isotopic sources (Sm-Nd) of Late Ediacaran series in the Iberian Massif: Implications for the Central Iberian-Ossa Morena boundary. Precambr. Res. 324, 194–207.

Rojo-Pérez, E., Fuenlabrada, J.M., Linnemann, U., Arenas, R., Sánchez Martínez, S., Díez Fernández, R., Martín Parra, L.M., Matas, J., Andonaegui, P., Fernández-Suárez, J., 2021. Geochemistry and Sm–Nd isotopic sources of Late Ediacaran siliciclastic series in the Ossa-Morena Complex: Iberian-Bohemian correlations. Int. J. Earth Sci. 110, 467–485.

Rojo-Pérez, E., Druguet, E., Casas, J.M., Proenza, J.A., Fuenlabrada, J.M., Sánchez Martínez, S., Garcia-Casco, A., Arenas, R., 2023. Geochemistry of metasedimentary rocks from the Eastern Pyrenees (Iberian Peninsula): Implications for correlation of Ediacaran terranes along the Gondwanan margin. Precambr. Res. 397, 107186. https://doi.org/10.1016/j.precamres.2023.107186.

Rosell, J., Arribas, J., 1989. Características petrológicas de las areniscas del Carbonífero de facies Culm de la isla de Menorca. Boletín Geológico y Minero De España 100, 853–864 (in Spanish).

Rosell, J., Gómez-Gras, D., Elizaga, E., 1987a. Mapa geologíco y memoria de la hoja 618 (Cap Menorca y Ciutadella) del Mapa Geológico de España. Instituto Geológico y Minero de España, Madrid (in Spanish).

Rosell, J., Gómez-Gras, D., Elizaga, E., 1987b. Mapa geologíco y memoria de la hoja 646 (Cala en Brut y Alaior) del Mapa Geológico de España. Instituto Geológico y Minero de España, Madrid (in Spanish).

Sabat, F., Gelabert, B., Rodriguez-Perea, A., 2018. Minorca, an exotic Balearic island (western Mediterranean). Geol. Acta 16, 411–426.

Sáinz de Baranda, B., Lunar Hernández, R., 1989. El volcanismo alcalino pre-Hercínico del sinclinal de Almaden. Estud. Geol. 45, 337–348.

Schulmann, K., Edel, J.B., Martínez Catalán, J.R., Mazur, S., Guy, A., Lardeaux, J.M., Ayarza, P., Palomeras, I., 2022. Tectonic evolution and global crustal architecture of the European Variscan belt constrained by geophysical data. Earth Sci. Rev. 234, 104195.

Shaw, J., Gutiérrez-Alonso, G., Johnston, S.T., Pastor-Galán, D., 2014. Provenance variability along the Early Ordovician north Gondwana margin: Paleogeographic and tectonic implications of U-Pb detrital zircon ages from the Armorican Quartzite of the Iberian Variscan belt. Geol. Soc. Am. Bull. 126, 702–719.

Stampfli, G.M., Borel, G.D., 2002. A plate tectonic model for the Paleozoic and Mesozoic constrained by dynamic plate boundaries and restored synthetic oceanic isochrons. Earth Planet. Sci. Lett. 196, 17–33.

Stampfli, G., Hochard, C., Vérard, C., Wilheim, C., vonRaumer, J., 2013. The formation of Pangea. Tectonophysics 593, 1–19.

Steiger, R.H., Jäger, E., 1977. Subcommission on geochronology: convention on the use of decay constants in geo-and cosmochronology. Earth Planet. Science Letters 36, 359–362.

Stephan, T., Kroner, U., Romer, R.L., Rösel, D., 2019. From a bipartite Gondwanan shelf to an arcuate Variscan belt: The early Paleozoic evolution of northern Peri-Gondwana. Earth Sci. Rev. 192, 491–512.

Stern, R.J., 2002. Crustal evolution in the East African Orogen: A neodymium isotopic perspective. Journal of African Earth Sciences 34, 109–117.

Sun, S-.S., Warren, R.G., Shaw, R.D., 1995. Nd isotope study of granites from the Arunta Inlier, central Australia: Constraints on geological models and limitation of the method. Precambrian Research 71, 301–314.

Tanaka, T., Togashi, S., Kamioka, H., Amakawa, H., Kagami, H., Hamamoto, T., Yuhara, M., Orihashi, Y., Yoneda, S., Shimizu, H., Kunimaru, T., Takahashi, K., Yanagi, T., Nakano, T., Fujimaki, H., Shinjo, R., Asahara, Y., Tanimizu, M., Dragusanu, C., 2000. JNdi-1: A neodymium isotopic reference in consistency with La Jolla neodymium. Chem. Geol. 168, 279–281.

Taylor, S.R., McLennan, S.M., 1985. The continental crust: Its composition and evolution. Blackwell, Oxford, p. 312.

Tiedt, C., 1994. Die Oberdevonsiche bis Unterkarbonische schichtfolge Menorcas (Balearen, Spanien). Ph.D. thesis, Institute of Geology and Paleontology, University of Hannover, 105 pp (in German).

Timoner, C., de Vicente, G., Olaiz, A., Díez-Fernández, R., 2021. Late Cenozoic left lateral strike-slip deformation in Minorca, Balearic Islands, Spain. Geotemas 18, 120–123.

White, W.M., 2013. Geochemistry. Wiley-Blackwell, 660 pp.

Winchester, J.A., Max, M.D., 1989. Tectonic setting discrimination in clastic sequences: An example from the late Proterozoic Erris Group, NW Ireland. Precambr. Res. 45, 191–201.